International Journal of Modern Physics A
Vol. 29, No. 2 (2014) 1430003 (25 pages)

DOI: 10.1142/S0217751X14300038

World Scientific
www.worldscientific.com



# TENTH-ORDER QED CONTRIBUTION TO THE ELECTRON $g-2$ AND HIGH PRECISION TEST OF QUANTUM ELECTRODYNAMICS*

TOICHIRO KINOSHITA

*Laboratory for Elementary Particle Physics,*
*Cornell University, Ithaca, New York 14853, USA*
*tk42@cornell.edu*

Received 15 December 2013
Accepted 18 December 2013
Published 13 January 2014

This paper presents the current status of the theory of electron anomalous magnetic moment $a_e \equiv (g-2)/2$, including a complete evaluation of 12,672 Feynman diagrams in the tenth-order perturbation theory. To solve this problem, we developed a code-generator which converts Feynman diagrams automatically into fully renormalized Feynman-parametric integrals. They are evaluated numerically by an integration routine VEGAS. The preliminary result obtained thus far is 9.16 (58) $(\alpha/\pi)^5$, where (58) denotes the uncertainty in the last two digits. This leads to $a_e(\text{theory}) = 1.159\ 652\ 181\ 78\ (77) \times 10^{-3}$, which is in agreement with the latest measurement $a_e(\exp:2008) = 1.159\ 652\ 180\ 73\ (28) \times 10^{-3}$. It shows that the Feynman–Dyson method of perturbative QED works up to the precision of $10^{-12}$.

*Keywords*: Electron anomalous magnetic moment; fine structure constant.

PACS numbers: 13.40.Em, 06.20.Jr, 12.20.Ds, 14.60.Cd

## 1. Introduction

An electron is a tiny magnet whose strength can be expressed as

$$g\frac{e}{2m}\frac{\hbar}{2}, \tag{1}$$

where $e$ and $m$ are the charge and mass of the electron, $\hbar$ is the Planck constant, and $g = 2$ according to the Dirac equation.[1,2]

Actually, it was found experimentally that $g$ is slightly larger than 2. The deviation of $g$ from 2, $a_e \equiv (g-2)/2$, is called anomalous magnetic moment. It became the subject of intense experimental and theoretical investigations.

*Invited talk at the conference in Honor of 90th Birthday of Freeman Dyson, Institute of Advanced Studies, Nanyang Technological University, Singapore, 26–29 August 2013.

Recent measurement of $a_e$ by the Harvard group in a cylindrical Penning trap has reached a very high precision[3,4]

$$a_{e^-}(\exp:2008) = 1.159\ 652\ 180\ 73\ (28) \times 10^{-3} \quad [0.24\ \text{ppb}]\,. \tag{2}$$

The uncertainty of this measurement is only four times larger than

$$\left(\frac{\alpha}{\pi}\right)^5 \sim 0.068 \times 10^{-12}\,, \tag{3}$$

where $\alpha$ is the fine structure constant. This means that it provides an opportunity for a very stringent test of the validity of QED and the Standard Model (SM).

Here, I will describe the theoretical work of our group which is competitive with the experimental uncertainty of (2) in precision and enables us to test the validity of QED to the tenth-order.

## 2. Brief Survey of Physics of Electron $g - 2$

Before describing our work on the tenth-order term, let me give a brief (and not exactly chronological) survey of how theory and experiment of electron $g - 2$ developed over the last 66 years, stimulating each other to higher and higher precision.

### 2.1. *Discovery of electron anomalous magnetic moment*

In 1947, the electron's $g$-factor was found to deviate from 2, the value given by the Dirac equation,[1,2] in the study of Zeeman splitting of Ga atom:[5]

$$a_e(\exp:1947) = 1.19\ (5) \times 10^{-3}\,. \tag{4}$$

Schwinger showed that it can be explained as a QED effect:[6,7]

$$a_e^{(2)}(\text{th}:1948) = \frac{\alpha}{2\pi} = 1.161\cdots \times 10^{-3} \tag{5}$$

using the renormalized QED, which was just discovered by Tomonaga[8,9] and Schwinger.[10]

Together with the Bethe's work on the hydrogen Lamb shift,[11] this provided the convincing evidence that (until then divergent) QED is the correct theory of electromagnetic interaction, provided that it is renormalized.

### 2.2. *Calculation of the fourth-order term of $a_e$*

In the renormalized QED $a_e$ can be written as a power series in $\alpha/\pi$:

$$A_1^{(2)}\left(\frac{\alpha}{\pi}\right) + A_1^{(4)}\left(\frac{\alpha}{\pi}\right)^2 + A_1^{(6)}\left(\frac{\alpha}{\pi}\right)^3 + \cdots\,, \tag{6}$$

where the coefficients $A_1^{(2)}$, etc. are finite because of renormalizability.

The result obtained by Schwinger corresponds to[6,7]

$$A_1^{(2)} = 0.5\,. \tag{7}$$

Naturally one wonders whether QED works beyond the second-order. The first attempt to analytic calculation of $A_1^{(4)}$ led to[12]

$$A_1^{(4)} = -2.97\,, \quad a_e(\text{th}:1950) = 1.147 \times 10^{-3}\,. \tag{8}$$

Unfortunately, this did not agree with the improved measurement[13]

$$a_e(\text{exp}:1956) = 1.168\ (5) \times 10^{-3}\,, \tag{9}$$

obtained using a new measurement of $\mu_p/\mu_0$, where $\mu_p$ is the magnetic moment of the proton and $\mu_0 = 4\pi \times 10^{-7} N A^{-1}$ is the magnetic permissivity of the vacuum.

Petermann[14] discovered by numerical integration, a sign error in one of the integrals contributing to (8). This led him to reevaluate the entire $A_1^{(4)}$. The correct analytic result was obtained by Petermann[15] and Sommerfield:[16]

$$\begin{aligned} A_1^{(4)} &= -0.328\ 478\ 965\ 579\ldots\,, \\ a_e(\text{th}:1957) &= 1.159\ 638\ (4) \times 10^{-3}\,, \end{aligned} \tag{10}$$

where the uncertainty comes from $\alpha$ available in 1957, which was known much more accurately than the theory and measurement of $a_e$.

### 2.3. *Feynman–Dyson method*

Note that this fourth-order calculation was carried out by the method of Feynman and Dyson, not by that of Schwinger or Tomonaga. This is because the unorthodox theory of Feynman,[17,18] whose equivalence with the Tomonaga–Schwinger theory was proved by Dyson,[19] gives a simpler and intuitive picture than the latter and enables us to calculate $g-2$ much more easily.

To highlight the difference of Feynman–Dyson (FD) method and that of Schwinger (or Tomonaga), let us recall how $A_1^{(2)}$ is calculated in the FD approach. It begins with drawing of a Feynman diagram as shown in Fig. 1.

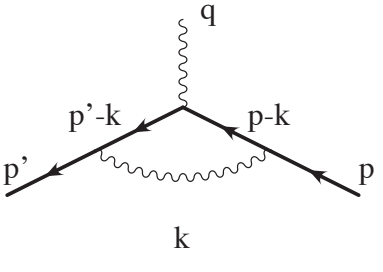


Fig. 1. Radiative correction to the scattering of an electron from momentum $p$ to momentum $p'$ by the potential (represented by $q$).

Then, apply the FD rules to this diagram and obtain

$$\lim_{\epsilon\to+0} \text{const} \times \int d^4k\, \bar{u}(p')\gamma^\lambda \frac{i}{\not{p}' - \not{k} - m + i\epsilon}\gamma^\mu \frac{i}{\not{p} - \not{k} - m + i\epsilon}\gamma^\nu u(p) \frac{-ig_{\lambda\nu}}{k^2 + i\epsilon}\,. \tag{11}$$

Integrating over the four-momentum variable $k$ and extracting the magnetic form factor, we obtain $A_1^{(2)}$. The whole calculation takes one or two sheets of paper.

In Schwinger's theory, each Feynman propagator is replaced by two related functions. Thus, Schwinger's starting formula for $A_1^{(2)}$ will be at least $2^3 = 8$ times longer than that of FD. (Actually, it is more complicated.)

The advantage of FD theory becomes even more evident in the fourth-order. Seven Feynman diagrams contribute to $A_1^{(4)}$, each diagram containing six Feynman propagators. Thus, Schwinger's starting formula for $A_1^{(4)}$ will be at least $2^6 = 64$ times longer than that of FD for each diagram.

### 2.4. *Direct measurement of $g - 2$ by spin precession*

While measurement of $g$ in atomic physics became stalled, an entirely different approach, measurement of $g - 2$ by spin precession in a magnetic field, pursued since $\sim$ 1953 by the University of Michigan group, has been making a steady progress.[20–22] After almost 20 years,[23] this method reached the precision of $\sim 3 \times 10^{-6}$

$$a_e(\exp:1971) = 1.159\ 6577\ (35) \times 10^{-3}\,. \tag{12}$$

This is 1400 times more precise than the atomic physics result $a_e(\exp:1956)$, forcing theorists to evaluate the sixth-order term $A_1^{(6)}$.

### 2.5. *Calculation of the sixth-order term of $a_e$*

Evaluation of $A_1^{(6)}$ requires 72 Feynman diagrams. Some diagrams were evaluated analytically in 1969–1975.[24–28] Others are more difficult to handle analytically. Thus, numerical integration approach was tried by several groups.[29,30] My own participation began around 1967.[31,32]

It took 25 years before numerical work produced sufficiently accurate $A_1^{(6)}$, primarily because of inadequate computing power then available.[33] Analytic work (also done on computer) took more than 30 years, too, leading to an exact result[34]

$$A_1^{(6)} = 1.181\ 241\ 456\ldots\,. \tag{13}$$

The numerical result is in good agreement with the analytic result within its uncertainty.

### 2.6. *Mass-dependent terms of $a_e$*

With such a precision, we must also take account of heavier particles such as muon, tau, hadrons and weak bosons. Assuming that muon and tau behave exactly like

electron in their interaction with the photon, we can express $a_e(\mathrm{QED})$ as

$$a_e(\mathrm{QED}) = A_1 + A_2\left(\frac{m_e}{m_\mu}\right) + A_2\left(\frac{m_e}{m_\tau}\right) + A_3\left(\frac{m_e}{m_\mu}, \frac{m_e}{m_\tau}\right). \tag{14}$$

The renormalizability means that $A_i$ can be written as a power series

$$A_i = A_i^{(2)}\left(\frac{\alpha}{\pi}\right) + A_i^{(4)}\left(\frac{\alpha}{\pi}\right)^2 + A_i^{(6)}\left(\frac{\alpha}{\pi}\right)^3 + \cdots, \quad i = 1, 2, 3, \tag{15}$$

with finite expansion coefficients.

$A_2$ and $A_3$ of fourth- and sixth-orders had been obtained analytically or as power series expansion in $m_e/m_\mu$ or $m_e/m_\tau$:[35–40]

$$\begin{aligned}
A_2^{(4)}\left(\frac{m_e}{m_\mu}\right) &= 5.197\ 386\ 67\ (26) \times 10^{-7}, \\
A_2^{(4)}\left(\frac{m_e}{m_\tau}\right) &= 1.837\ 98\ (34) \times 10^{-9}, \\
A_2^{(6)}\left(\frac{m_e}{m_\mu}\right) &= -7.373\ 941\ 55\ (27) \times 10^{-6}, \\
A_2^{(6)}\left(\frac{m_e}{m_\tau}\right) &= -6.5830\ (11) \times 10^{-8}, \\
A_3^{(6)}\left(\frac{m_e}{m_\mu}, \frac{m_e}{m_\tau}\right) &= 1.909\ (1) \times 10^{-13}.
\end{aligned} \tag{16}$$

The uncertainties are due only to those of measured mass ratios $m_e/m_\mu$ or $m_e/m_\tau$.

The contributions of hadrons and weak bosons are more complicated but can be evaluated within the framework of SM. At present, the hadronic term is derived mostly from the experimental data related to the hadronic vacuum polarization. (Theory of QCD is not yet ready.)

Latest evaluations of hadronic contributions are[41,42]

$$\begin{aligned}
a_e(\text{had. v.p.}) &= 1.866\ (10)_{\mathrm{exp}}\ (5)_{\mathrm{rad}} \times 10^{-12}, \\
a_e(\text{NLO had. v.p.}) &= -0.2234\ (12)_{\mathrm{exp}}\ (7)_{\mathrm{rad}} \times 10^{-12}, \\
a_e(\text{had. l-l}) &= 0.035\ (10) \times 10^{-12}.
\end{aligned} \tag{17}$$

The electroweak contribution is small but not negligible:[43–46]

$$a_e(\mathrm{EW}) = 0.0297\ (5) \times 10^{-12}. \tag{18}$$

### 2.7. *Some high precision measurements of α*

Now that the precision of $a_e(\mathrm{exp}:1971)$ and $a_e(\mathrm{th})$ evaluated with $A_1^{(6)}$ of (13) becomes very high so that a more accurate value of $\alpha$ is required for their comparison.

Following are some of such $\alpha$ that became available:[47]

$$\begin{aligned}
\alpha^{-1}(\text{ac Josephson}) &= 137.035\ 9875\ (43) \quad [31\ \text{ppb}]\,,\\
\alpha^{-1}(\text{quantum Hall}) &= 137.036\ 0030\ (25) \quad [18\ \text{ppb}]\,,\\
\alpha^{-1}(\text{neutron wavelength}) &= 137.036\ 0077\ (28) \quad [21\ \text{ppb}]\,,\\
\alpha^{-1}(\text{atom interferometry}) &= 137.036\ 0000\ (11) \quad [7.7\ \text{ppb}]\,,\\
\alpha^{-1}(\text{optical lattice}) &= 137.035\ 998\ 83\ (91) \quad [6.7\ \text{ppb}]\,.
\end{aligned} \tag{19}$$

### 2.8. *Penning trap method*

While the spin precession method hits the ceiling, an approach that utilizes the spin and cyclotron resonances in a Penning trap (which began $\sim$1958) was being pursued by the group at the University of Washington.[48,49] After $\sim$30 years this approach led to three orders of magnitude improvement over the precession measurement of Michigan group. Their results for an electron and positron are[50]

$$\begin{aligned}
a_{e^-}(\exp:1987) &= 1.159\ 652\ 1884\ (43)\times 10^{-3}\,,\\
a_{e^+}(\exp:1987) &= 1.159\ 652\ 1879\ (43)\times 10^{-3}\,.
\end{aligned} \tag{20}$$

This means that theory must be extended to the eighth-order since

$$\left(\frac{\alpha}{\pi}\right)^4 \sim 29\times 10^{-12}\,. \tag{21}$$

### 2.9. *Numerical evaluation of $a_e$ in the eighth-order*

Evaluation of $A_1^{(8)}$ requires 891 Feynman diagrams. Only numerical integration results are available at present. The value of $A_1^{(8)}$ obtained after more than 20 years of work was published recently:[51,52,63]

$$A_1^{(8)} = -1.9106\ (20)\,. \tag{22}$$

Further reduction of uncertainty in $A_1^{(8)}$ is in progress.

$A_2^{(8)}$ and $A_3^{(8)}$ have also been evaluated:[52,a]

$$\begin{aligned}
A_2^{(8)}\left(\frac{m_e}{m_\mu}\right) &= 9.222\ (66)\times 10^{-4}\,,\\
A_2^{(8)}\left(\frac{m_e}{m_\tau}\right) &= 7.38\ (12)\times 10^{-6}\,,\\
A_3^{(8)}\left(\frac{m_e}{m_\mu},\frac{m_e}{m_\tau}\right) &= 7.465\ (18)\times 10^{-7}\,.
\end{aligned} \tag{23}$$

[a]A copying error in the value of one of the integrals contributing to $A_2^{(8)}(m_e/m_\tau)$ was pointed out in a paper (to be published) by Kurz, Lin, Marquard and Steinhauser. I thank them for correcting this error. The second term in (23) includes this correction.

### 2.10. *Numerical evaluation of $a_e$ in the tenth-order*

As was mentioned in Sec. 1 the Harvard measurement of $a_e$, which is $\sim$15 times more precise than the University of Washington measurement (20), demands the knowledge of $A_1^{(10)}$, which requires evaluation of 12,672 Feynman diagrams. In anticipation of the forthcoming Harvard measurement, we began working on the tenth-order around 2003.[66]

After only eight years of work, we obtained a preliminary result[52]

$$A_1^{(10)} = 9.16\ (58)\,. \tag{24}$$

This is still very preliminary. Further work is in progress.

$A_2^{(10)}$ has also been evaluated:[52]

$$A_2^{(10)}\left(\frac{m_e}{m_\mu}\right) = -0.003\ 82\ (39)\,. \tag{25}$$

To evaluate $a_e$ precisely, we need $\alpha$ better than those listed in (19). Such an $\alpha$ at present is the one based on Bloch oscillation and atom interferometry:[53,54]

$$\alpha^{-1}(\mathrm{Rb11}) = 137.035\ 999\ 049\ (90) \quad [0.66\ \mathrm{ppb}]\,. \tag{26}$$

Using this $\alpha$, we obtain

$$a_e(\mathrm{th{:}2012}) = 1.159\ 652\ 181\ 78\ (6)(4)(2)(77) \times 10^{-3} \quad [0.66\ \mathrm{ppb}]\,, \tag{27}$$

where the uncertainties are from the eighth-order term, tenth-order term, hadronic and electroweak terms, and $\alpha(\mathrm{Rb11})$, respectively. This is in reasonable agreement with the measured $a_e$:

$$a_e(\mathrm{exp{:}2008}) - a_e(\mathrm{th{:}2012}) = -1.05\ (82) \times 10^{-12}\,. \tag{28}$$

Note that the largest uncertainty in (24) comes from $\alpha(\mathrm{Rb11})$. In other words, non-QED $\alpha$, even the best one available at present, is too crude to test QED to the extent achieved by theory and measurement of $a_e$. Thus, it makes more sense to test QED by an alternative approach, namely, obtain $\alpha$ from $a_e$ and compare it with other $\alpha$'s. This leads to

$$\alpha^{-1}(a_e) = 137.035\ 999\ 1727\ (68)(46)(19)(331) \quad [0.25\ \mathrm{ppb}]\,, \tag{29}$$

where 68, 46, 19, 331 are uncertainties of eighth-order, tenth-order, hadronic and electroweak, and from the measurement of $a_e(\mathrm{exp{:}2008})$.

## 3. Summary: Current Status

- Comparison of $a_e$(theory) and $a_e$(experiment)

$$\begin{aligned} a_e(\mathrm{exp{:}2008}) &= 1.159\ 652\ 180\ 73\ (28) \times 10^{-3} && [0.24\ \mathrm{ppb}]\,, \\ a_e(\mathrm{th{:}2012}) &= 1.159\ 652\ 181\ 78\ (6)(4)(2)(77) \times 10^{-3} && [0.66\ \mathrm{ppb}]\,, \\ a_e(\mathrm{exp{:}2008}) &- a_e(\mathrm{th{:}2012}) = -1.05\ (82) \times 10^{-12}\,. \end{aligned} \tag{30}$$

The largest uncertainty $0.77 \times 10^{-12}$ in $a_e(\text{th}:2012)$ comes from $\alpha(\text{Rb11})$. The intrinsic theoretical uncertainty is $0.07 \times 10^{-12}$. This is four times smaller than the uncertainty $0.28 \times 10^{-12}$ of $a_e(\text{exp}:2008)$.

- Comparison of $\alpha(\text{Rb11})$ and $\alpha(a_e)$

$$\begin{aligned} \alpha^{-1}(\text{Rb11}) &= 137.035\ 999\ 049\ (90) && [0.66\ \text{ppb}]\,, \\ \alpha^{-1}(a_e) &= 137.035\ 999\ 1727\ (68)(46)(19)(331) && [0.25\ \text{ppb}]\,, \\ \alpha^{-1}(\text{Rb11}) - \alpha^{-1}(a_e) &= -0.124\ (96) \times 10^{-6}\,. \end{aligned} \tag{31}$$

Note that $\alpha^{-1}(a_e)$ is 2.6 times more precise than $\alpha^{-1}(\text{Rb11})$, and that the uncertainty of $\alpha^{-1}(a_e)$ is dominated by the uncertainty in the measurement of $a_e(\text{exp}:2008)$.

## 4. Evaluation of Tenth-Order Term: How is it Done?

Now, let me sketch how 12,672 Feynman diagrams that contribute to $A_1^{(10)}$ were evaluated. This is really a gigantic project, requiring a systematic and highly organized approach.

Fortunately, the numerical renormalization method developed in 1974 for the sixth-order case[62] and updated for the eighth-order case[63] turned out to be readily adaptable to automation.

The first step is to classify them into gauge-invariant sets. We find 32 gauge-invariant sets shown in Fig. 2.

### 4.1. *Numerical renormalization of integrals*

Only a small fraction of tenth-order diagrams have been evaluated analytically.[64] (Recall: Even eighth-order is not yet done.) Thus, the numerical approach is the only viable option at present. We carry out numerical integration by VEGAS, an iterative–adaptive routine based on random sampling of integrand.[65]

It is important to note that numerical method does not work if the integral is divergent, which may arise from large momentum region (UV) and/or vanishing of photon momenta (IR). Our integrals are full of these divergences which must be removed by carrying out renormalization for the integrand, namely, *before* they are integrated.

### 4.2. *Reducing the number of integrals*

Another problem we have to deal with is the large number of diagrams. The combined uncertainty $\sigma_N$ of $N$ independent integrals will grow roughly as $\sqrt{N}$. This means that $\sigma_N$ becomes large for large $N$, even if each integral has small uncertainty. This is particularly troublesome for the Set V, which is a set of Feynman diagrams represented by the diagram denoted $V$ in Fig. 2, for which $N = 6354$. We tried to alleviate this problem with the help of Ward–Takahashi identity.

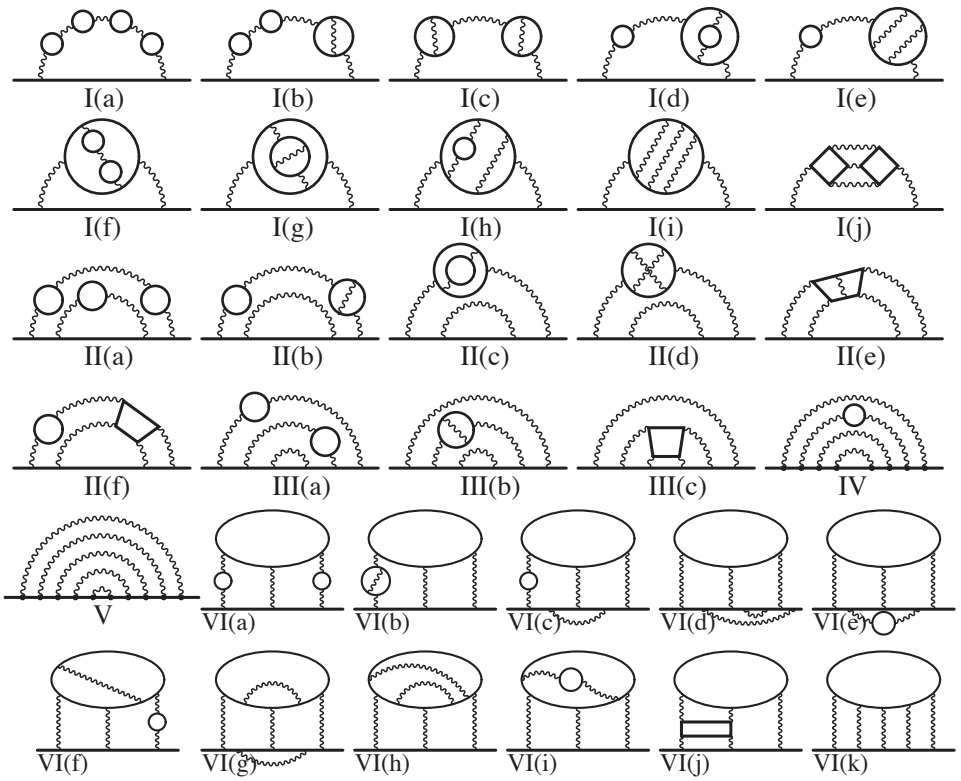


Fig. 2. Diagrams of 32 gauge-invariant sets contributing to the tenth-order lepton $g-2$ represented by their respective self-energy-like diagrams. Solid lines represent lepton lines propagating in a weak magnetic field.

Let $\Sigma(p)$ be a self-energy type diagram without closed electron loop, and let $\Lambda^{\nu}(p,q)$ be the sum of nine vertex diagrams which are derived from $\Sigma(p)$ by inserting an external vertex in all electron lines. Rewrite this sum as

$$\Lambda^{\nu}(p,q) \simeq -q_{\mu}\left[\frac{\partial\Lambda_{\mu}(p,q)}{\partial q_{\nu}} - \frac{\partial\Sigma(p)}{\partial p_{\nu}}\right]_{q=0}, \tag{32}$$

using the Ward–Takahashi identity, and evaluate the right-hand side. This has the effect of compressing nine integrals into one. Furthermore, the code of the right-hand side is not much larger than that of the individual vertex term.

This enables us to cut the number of independent integrals to $6354/9 = 706$. Time reversal symmetry reduces it to 389. They are shown in Fig. 3.

### 4.3. *Automatic code generation*

These integrals have enormous size and complicated structure. It would thus be very difficult to obtain a FORTRAN code without making algebraic error, unless the derivation of the integral from the diagram is automated as much as possible.

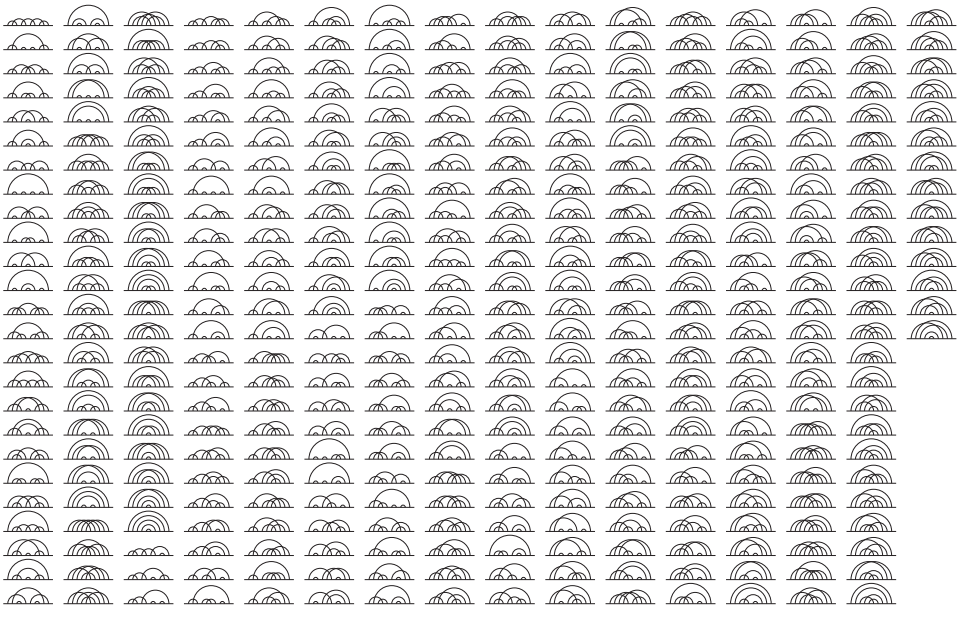

Fig. 3. 389 self-energy-like diagrams representing 6354 vertex diagrams of Set V. Each diagram represents 9 (or 18) vertex diagrams. The horizontal solid lines represent electron propagators in a constant weak magnetic field. Semicircles stand for photon propagators. The left-most figures are denoted as X001–X025 from top to bottom. The top figure second from left is denoted X026, and so on.

To deal with the Set V, in particular, we developed an automatic code generator GENCODE$N$, which converts these diagrams into integrals in several steps.[59,60]

### 4.4. *Preparation*: *Diagram identification*

Diagrams of Set V, which have no closed lepton loop, can be specified completely by the way vertices are connected by virtual photons $a$, $b$, $c$, $d$ and $e$. For instance the diagram X001 at the top-left corner of Fig. 3 is specified by the statement: *abacbdcede*, which means that vertices 1 and 3 (from the left end) are connected by the photon $a$, etc. In other words, this diagram can be represented by a file X001 consisting of this one line code. Similarly, all diagrams of Set V can be represented by the files X$abc$ ($abc = 001, 002, \ldots, 389$) which contain one-line code of their own.

Important: This sequence defines not only the diagram itself, but also identifies all UV- and IR-divergent subdiagrams.

### 4.5. *Step* 1: *Construction of unrenormalized integrand*

Translate "X$abc$" into momentum integral by the FD rules (using Perl). The output serves as an input for home-made analytic integration table written in FORM[61]

which turns it into an integral of the form

$$\int (dz) f(z)\,, \quad (dz) = \prod_{i=1}^{14} dz_i\, \delta\left(1 - \sum_{i=1}^{14} z_i\right). \tag{33}$$

$f(z)$ is a very complicated function of $z$ and seems nearly intractable. However, in terms of "building blocks" $B_{ij}$, $A_i$, $U$, $V$, it exhibits a well-organized structure

$$f(z) = \frac{F_0(B_{ij}, A_i)}{U^2 V^5} + \frac{F_1(B_{ij}, A_i)}{U^3 V^4} + \cdots . \tag{34}$$

### 4.6. *Step* 2: *Construction of building blocks*

GENCODE$N$ expresses $B_{ij}$ and $U$ as polynomials of $z_1$, $z_2, \ldots, z_{14}$. They are determined by the network topology of loop momenta, and obtained automatically by MAPLE (or FORM[61]) for each X$abc$.

$A_i$ is the fraction of external momentum flowing in the line $i$, and satisfies the Kirchhoff's loop law and junction law for "currents." The explicit form is

$$A_i = -\frac{1}{U} \sum_{j}^{\text{electron only}} z_j \left(B_{ij} - \delta_{ij} \frac{U}{z_j}\right). \tag{35}$$

$V$ has a form common to all diagrams of Set V:

$$V = \sum_{j}^{\text{electron only}} z_j (1 - A_j) m^2\,, \tag{36}$$

where $m$ is the electron mass.

### 4.7. *Step* 3: *Removal of UV divergences*

Our method of renormalization is to remove the divergence of integrand by subtraction before integration is carried out. UV divergence arises from a subdiagram $S$, which is identified by

$$U \to 0 \quad \text{for} \quad \sum_{S} z_i \to 0\,. \tag{37}$$

The UV subtraction term is built from the original integrand by K-operation,[59] which gives the UV limits of $B_{ij}$, $A_i$, $U$, $V$ based on a simple power-counting rule.

The properties of terms created by the K-operation:

- Point-wise subtraction of UV divergence.
- Subtraction term factorizes analytically into a product of UV-divergent piece and magnetic moment factor of lower-orders.
- The UV-divergent pieces $\delta m_n^{\text{UV}}$, $L_n^{\text{UV}}$, $B_n^{\text{UV}}$ differ from the actual renormalization constants $\delta m_n$, $L_n$, $B_n$ by UV-finite amounts.

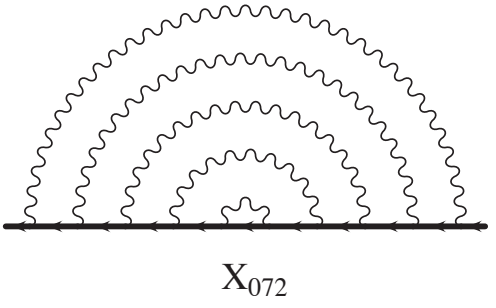


Fig. 4. Diagram X072 of Set V.

### 4.8. *Step* 4: *Removal of IR divergences*

Integrals still suffer from IR divergence, logarithmic or worse, which is characterized by $V \to 0$ in some subdomain of integration.

Linear (or worse) IR divergence is caused by the UV-finite part of $\delta m_n$: $\widetilde{\delta m_n} \equiv \delta m_n - \delta m_n^{\rm UV}$ $(n > 2)$.

This divergence can be removed by subtracting $\widetilde{\delta m_n}$ together with the UV-divergent part $\delta m_n^{\rm UV}$ so that full mass renormalization is achieved in Step 3.

The remaining logarithmic IR divergence can be handled by point-wise subtraction and I-operation defined by the IR power counting.[60]

Actually some IR terms of the diagrams X253 and X256 were found to require a treatment not included in the IR subtraction rule of GENCODE*N* developed for the eighth-order diagrams. These are corrected by hand.[55]

### 4.9. *An example*: *Diagram X*072

As an example of these steps let us consider the diagram X072 (see Fig. 4).

The preliminary step produces a file that contains a one-line statement

$$abcdeedcba\,, \tag{38}$$

which identifies the order of vertices where photons $a$, $b$, $c$, $d$, $e$ are attached.

When this information is fed into GENCODE*N*, it generates a complete instruction for Steps 1 and 2 for building unrenormalized integral $M_{072}$ for the diagram X072 as well as Steps 3 and 4 for building 134 UV-divergent and IR-divergent subtraction integrals. (Note that the K-operation on a self-energy subdiagram creates two terms, one of $\delta m_n^{\rm UV}$ type and another of $B_n^{\rm UV}$ type.)

The finite term $\Delta M_{072}$ is defined by subtracting 242 terms of UV- and/or IR-divergent types from $M_{072}$ as shown below

$$\begin{aligned}\Delta M_{072} = M_{072} &- dm_{47}^{\rm UV} M_{2^*} - B_{47}^{\rm UV} M_2 - dm_{6b}^{\rm UV} M_{4b(2^*)} - B_{6b}^{\rm UV} M_{4b} \\ &- dm_{4b}^{\rm UV} M_{6b(3^*)} - B_{4b}^{\rm UV} M_{6b} - dm_2^{\rm UV} M_{47(4^*)} - B_2^{\rm UV} M_{47} \\ &+ dm_{6b}^{\rm UV} dm_{2^*}^{\rm UV} M_{2^*} + B_{6b}^{\rm UV} dm_{2(1')}^{\rm UV} M_{2^*} + B_{6b}^{\rm UV} B_{2(1')}^{\rm UV} M_2\end{aligned}$$

$$
\begin{aligned}
&+ dm_{4b}^{\mathrm{UV}} dm_{4b(2^*)}^{\mathrm{UV}} M_{2^*} + B_{4b}^{\mathrm{UV}} B_{4b(2')}^{\mathrm{UV}} M_2 + B_{4b}^{\mathrm{UV}} dm_{4b(2')}^{\mathrm{UV}} M_{2^*} \\
&+ dm_2^{\mathrm{UV}} dm_{6b(3^*)}^{\mathrm{UV}} M_{2^*} + B_2^{\mathrm{UV}} dm_{6b(3')}^{\mathrm{UV}} M_{2^*} + B_2^{\mathrm{UV}} B_{6b(3')}^{\mathrm{UV}} M_2 \\
&+ dm_{4b}^{\mathrm{UV}} dm_{2^*}^{\mathrm{UV}} M_{4b(2^*)} + B_{4b}^{\mathrm{UV}} dm_{2(1')}^{\mathrm{UV}} M_{4b(2^*)} + B_{4b}^{\mathrm{UV}} B_{2(1')}^{\mathrm{UV}} M_{4b} \\
&+ dm_2^{\mathrm{UV}} dm_{4b(2^*)}^{\mathrm{UV}} M_{4b(2^*)} + B_2^{\mathrm{UV}} dm_{4b(2')}^{\mathrm{UV}} M_{4b(2^*)} + B_2^{\mathrm{UV}} B_{4b(2')}^{\mathrm{UV}} M_{4b} \\
&+ dm_2^{\mathrm{UV}} dm_{2^*}^{\mathrm{UV}} M_{6b(3^*)} + B_2^{\mathrm{UV}} dm_{2(1')}^{\mathrm{UV}} M_{6b(3^*)} + B_2^{\mathrm{UV}} B_{2(1')}^{\mathrm{UV}} M_{6b} \\
&- dm_{4b}^{\mathrm{UV}} dm_{2^*}^{\mathrm{UV}} dm_{2^*}^{\mathrm{UV}} M_{2^*} - B_{4b}^{\mathrm{UV}} dm_{2(1')}^{\mathrm{UV}} dm_{2^*}^{\mathrm{UV}} M_{2^*} \\
&- B_{4b}^{\mathrm{UV}} B_{2(1')}^{\mathrm{UV}} dm_{2(1')}^{\mathrm{UV}} M_{2^*} - B_{4b}^{\mathrm{UV}} B_{2(1')}^{\mathrm{UV}} B_{2(1')}^{\mathrm{UV}} M_2 \\
&- B_2^{\mathrm{UV}} dm_{4b(2')}^{\mathrm{UV}} dm_{2^*}^{\mathrm{UV}} M_{2^*} - B_2^{\mathrm{UV}} B_{4b(2')}^{\mathrm{UV}} dm_{2(1')}^{\mathrm{UV}} M_{2^*} \\
&- B_2^{\mathrm{UV}} B_{4b(2')}^{\mathrm{UV}} B_{2(1')}^{\mathrm{UV}} M_2 - dm_2^{\mathrm{UV}} dm_{2^*}^{\mathrm{UV}} dm_{4b(2^*)}^{\mathrm{UV}} M_{2^*} \\
&- dm_2^{\mathrm{UV}} dm_{4b(2^*)}^{\mathrm{UV}} dm_{2^*}^{\mathrm{UV}} M_{2^*} - B_2^{\mathrm{UV}} dm_{2(1')}^{\mathrm{UV}} dm_{4b(2^*)}^{\mathrm{UV}} M_{2^*} \\
&- B_2^{\mathrm{UV}} B_{2(1')}^{\mathrm{UV}} dm_{4b(2')}^{\mathrm{UV}} M_{2^*} - B_2^{\mathrm{UV}} B_{2(1')}^{\mathrm{UV}} B_{4b(2')}^{\mathrm{UV}} M_2 \\
&- dm_2^{\mathrm{UV}} dm_{2^*}^{\mathrm{UV}} dm_{2^*}^{\mathrm{UV}} M_{4b(2^*)} - B_2^{\mathrm{UV}} dm_{2(1')}^{\mathrm{UV}} dm_{2^*}^{\mathrm{UV}} M_{4b(2^*)} \\
&- B_2^{\mathrm{UV}} B_{2(1')}^{\mathrm{UV}} B_{2(1')}^{\mathrm{UV}} M_{4b} + dm_2^{\mathrm{UV}} dm_{2^*}^{\mathrm{UV}} dm_{2^*}^{\mathrm{UV}} dm_{2^*}^{\mathrm{UV}} M_{2^*} \\
&- B_2^{\mathrm{UV}} B_{2(1')}^{\mathrm{UV}} dm_{2(1')}^{\mathrm{UV}} M_{4b(2^*)} + B_2^{\mathrm{UV}} dm_{2(1')}^{\mathrm{UV}} dm_{2^*}^{\mathrm{UV}} dm_{2^*}^{\mathrm{UV}} M_{2^*} \\
&+ B_2^{\mathrm{UV}} B_{2(1')}^{\mathrm{UV}} dm_{2(1')}^{\mathrm{UV}} dm_{2^*}^{\mathrm{UV}} M_{2^*} + B_{4b}^{\mathrm{UV}} dm_{4b(2')}^{\mathrm{R}} M_{2^*} \\
&+ B_2^{\mathrm{UV}} B_{2(1')}^{\mathrm{UV}} B_{2(1')}^{\mathrm{UV}} dm_{2(1')}^{\mathrm{UV}} M_{2^*} + B_2^{\mathrm{UV}} B_{2(1')}^{\mathrm{UV}} B_{2(1')}^{\mathrm{UV}} B_{2(1')}^{\mathrm{UV}} M_2 \\
&- dm_{47}^{\mathrm{R}} M_{2^*} + dm_{6b}^{\mathrm{UV}} dm_{2^*}^{\mathrm{R}} M_{2^*} + B_{6b}^{\mathrm{UV}} dm_{2(1')}^{\mathrm{R}} M_{2^*} \\
&+ dm_{4b}^{\mathrm{UV}} dm_{4b(2^*)}^{\mathrm{R}} M_{2^*} + dm_2^{\mathrm{UV}} dm_{6b(3^*)}^{\mathrm{R}} M_{2^*} + B_2^{\mathrm{UV}} dm_{6b(3')}^{\mathrm{R}} M_{2^*} \\
&- dm_{4b}^{\mathrm{UV}} dm_{2^*}^{\mathrm{UV}} dm_{2^*}^{\mathrm{R}} M_{2^*} - B_{4b}^{\mathrm{UV}} dm_{2(1')}^{\mathrm{UV}} dm_{2^*}^{\mathrm{R}} M_{2^*} \\
&- B_{4b}^{\mathrm{UV}} B_{2(1')}^{\mathrm{UV}} dm_{2(1')}^{\mathrm{R}} M_{2^*} - dm_2^{\mathrm{UV}} dm_{4b(2^*)}^{\mathrm{UV}} dm_{2^*}^{\mathrm{R}} M_{2^*} \\
&- B_2^{\mathrm{UV}} dm_{4b(2')}^{\mathrm{UV}} dm_{2^*}^{\mathrm{R}} M_{2^*} - B_2^{\mathrm{UV}} B_{4b(2')}^{\mathrm{UV}} dm_{2(1')}^{\mathrm{R}} M_{2^*} \\
&- dm_2^{\mathrm{UV}} dm_{2^*}^{\mathrm{UV}} dm_{4b(2^*)}^{\mathrm{R}} M_{2^*} - B_2^{\mathrm{UV}} dm_{2(1')}^{\mathrm{UV}} dm_{4b(2^*)}^{\mathrm{R}} M_{2^*} \\
&- B_2^{\mathrm{UV}} B_{2(1')}^{\mathrm{UV}} dm_{4b(2')}^{\mathrm{R}} M_{2^*} + dm_2^{\mathrm{UV}} dm_{2^*}^{\mathrm{UV}} dm_{2^*}^{\mathrm{UV}} dm_{2^*}^{\mathrm{R}} M_{2^*} \\
&+ B_2^{\mathrm{UV}} dm_{2(1')}^{\mathrm{UV}} dm_{2^*}^{\mathrm{UV}} dm_{2^*}^{\mathrm{R}} M_{2^*} + B_2^{\mathrm{UV}} B_{2(1')}^{\mathrm{UV}} dm_{2(1')}^{\mathrm{UV}} dm_{2^*}^{\mathrm{R}} M_{2^*} \\
&+ B_2^{\mathrm{UV}} B_{2(1')}^{\mathrm{UV}} B_{2(1')}^{\mathrm{UV}} dm_{2(1')}^{\mathrm{R}} M_{2^*} - M_{47} L_{2v}^{\mathrm{R}} + dm_{6b}^{\mathrm{UV}} M_{2^*} L_{2v}^{\mathrm{R}} \\
&+ B_{6b}^{\mathrm{UV}} M_2 L_{2v}^{\mathrm{R}} + dm_{4b}^{\mathrm{UV}} M_{4b(2^*)} L_{2v}^{\mathrm{R}} + B_{4b}^{\mathrm{UV}} M_{4b} L_{2v}^{\mathrm{R}}
\end{aligned}
$$

$$
\begin{aligned}
&+ dm_2^{\mathrm{UV}} M_{6b(3^*)} L_{2v}^{\mathrm{R}} - B_{4b}^{\mathrm{UV}} B_{2(1')}^{\mathrm{UV}} M_2 L_{2v}^{\mathrm{R}} + B_2^{\mathrm{UV}} M_{6b} L_{2v}^{\mathrm{R}} \\
&- dm_{4b}^{\mathrm{UV}} dm_{2^*}^{\mathrm{UV}} M_{2^*} L_{2v}^{\mathrm{R}} - B_{4b}^{\mathrm{UV}} dm_{2(1')}^{\mathrm{UV}} M_{2^*} L_{2v}^{\mathrm{R}} \\
&- dm_2^{\mathrm{UV}} dm_{4b(2^*)}^{\mathrm{UV}} M_{2^*} L_{2v}^{\mathrm{R}} - B_2^{\mathrm{UV}} dm_{4b(2')}^{\mathrm{UV}} M_{2^*} L_{2v}^{\mathrm{R}} \\
&- B_2^{\mathrm{UV}} B_{4b(2')}^{\mathrm{UV}} M_2 L_{2v}^{\mathrm{R}} - dm_2^{\mathrm{UV}} dm_{2^*}^{\mathrm{UV}} M_{4b(2^*)} L_{2v}^{\mathrm{R}} \\
&- B_2^{\mathrm{UV}} dm_{2(1')}^{\mathrm{UV}} M_{4b(2^*)} L_{2v}^{\mathrm{R}} - B_2^{\mathrm{UV}} B_{2(1')}^{\mathrm{UV}} M_{4b} L_{2v}^{\mathrm{R}} \\
&+ dm_2^{\mathrm{UV}} dm_{2^*}^{\mathrm{UV}} dm_{2^*}^{\mathrm{UV}} M_{2^*} L_{2v}^{\mathrm{R}} + B_2^{\mathrm{UV}} dm_{2(1')}^{\mathrm{UV}} dm_{2^*}^{\mathrm{UV}} M_{2^*} L_{2v}^{\mathrm{R}} \\
&+ B_2^{\mathrm{UV}} B_{2(1')}^{\mathrm{UV}} dm_{2(1')}^{\mathrm{UV}} M_{2^*} L_{2v}^{\mathrm{R}} + B_2^{\mathrm{UV}} B_{2(1')}^{\mathrm{UV}} B_{2(1')}^{\mathrm{UV}} M_2 L_{2v}^{\mathrm{R}} \\
&- dm_{6b}^{\mathrm{R}} M_{4b(2^*)} + dm_{6b}^{\mathrm{R}} dm_{2^*}^{\mathrm{UV}} M_{2^*} + dm_{4b}^{\mathrm{UV}} dm_{2^*}^{\mathrm{R}} M_{4b(2^*)} \\
&+ B_{4b}^{\mathrm{UV}} dm_{2(1')}^{\mathrm{R}} M_{4b(2^*)} + dm_2^{\mathrm{UV}} dm_{4b(2^*)}^{\mathrm{R}} M_{4b(2^*)} \\
&+ B_2^{\mathrm{UV}} dm_{4b(2')}^{\mathrm{R}} M_{4b(2^*)} - dm_{4b}^{\mathrm{UV}} dm_{2^*}^{\mathrm{R}} dm_{2^*}^{\mathrm{UV}} M_{2^*} \\
&- B_{4b}^{\mathrm{UV}} dm_{2(1')}^{\mathrm{R}} dm_{2^*}^{\mathrm{UV}} M_{2^*} - dm_2^{\mathrm{UV}} dm_{4b(2^*)}^{\mathrm{R}} dm_{2^*}^{\mathrm{UV}} M_{2^*} \\
&- B_2^{\mathrm{UV}} dm_{4b(2')}^{\mathrm{R}} dm_{2^*}^{\mathrm{UV}} M_{2^*} - dm_2^{\mathrm{UV}} dm_{2^*}^{\mathrm{UV}} dm_{2^*}^{\mathrm{R}} M_{4b(2^*)} \\
&- B_2^{\mathrm{UV}} dm_{2(1')}^{\mathrm{UV}} dm_{2^*}^{\mathrm{R}} M_{4b(2^*)} - B_2^{\mathrm{UV}} B_{2(1')}^{\mathrm{UV}} dm_{2(1')}^{\mathrm{R}} M_{4b(2^*)} \\
&+ dm_2^{\mathrm{UV}} dm_{2^*}^{\mathrm{UV}} dm_{2^*}^{\mathrm{R}} dm_{2^*}^{\mathrm{UV}} M_{2^*} + B_2^{\mathrm{UV}} dm_{2(1')}^{\mathrm{UV}} dm_{2^*}^{\mathrm{R}} dm_{2^*}^{\mathrm{UV}} M_{2^*} \\
&+ B_2^{\mathrm{UV}} B_{2(1')}^{\mathrm{UV}} dm_{2(1')}^{\mathrm{R}} dm_{2^*}^{\mathrm{UV}} M_{2^*} - M_{6b} L_{4b2v}^{\mathrm{R}} + M_{6b} L_{2v}^{\mathrm{UV}} L_{2v}^{\mathrm{R}} \\
&+ dm_{4b}^{\mathrm{UV}} M_{2^*} L_{4b2v}^{\mathrm{R}} + B_{4b}^{\mathrm{UV}} M_2 L_{4b2v}^{\mathrm{R}} + dm_2^{\mathrm{UV}} M_{4b(2^*)} L_{4b2v}^{\mathrm{R}} \\
&+ B_2^{\mathrm{UV}} M_{4b} L_{4b2v}^{\mathrm{R}} - dm_{4b}^{\mathrm{UV}} M_{2^*} L_{2v}^{\mathrm{UV}} L_{2v}^{\mathrm{R}} - B_{4b}^{\mathrm{UV}} M_2 L_{2v}^{\mathrm{UV}} L_{2v}^{\mathrm{R}} \\
&- dm_2^{\mathrm{UV}} M_{4b(2^*)} L_{2v}^{\mathrm{UV}} L_{2v}^{\mathrm{R}} - B_2^{\mathrm{UV}} M_{4b} L_{2v}^{\mathrm{UV}} L_{2v}^{\mathrm{R}} \\
&- dm_2^{\mathrm{UV}} dm_{2^*}^{\mathrm{UV}} M_{2^*} L_{4b2v}^{\mathrm{R}} - B_2^{\mathrm{UV}} dm_{2(1')}^{\mathrm{UV}} M_{2^*} L_{4b2v}^{\mathrm{R}} \\
&- B_2^{\mathrm{UV}} B_{2(1')}^{\mathrm{UV}} M_2 L_{4b2v}^{\mathrm{R}} + dm_2^{\mathrm{UV}} dm_{2^*}^{\mathrm{UV}} M_{2^*} L_{2v}^{\mathrm{UV}} L_{2v}^{\mathrm{R}} \\
&+ B_2^{\mathrm{UV}} dm_{2(1')}^{\mathrm{UV}} M_{2^*} L_{2v}^{\mathrm{UV}} L_{2v}^{\mathrm{R}} + B_2^{\mathrm{UV}} B_{2(1')}^{\mathrm{UV}} M_2 L_{2v}^{\mathrm{UV}} L_{2v}^{\mathrm{R}} \\
&- dm_{4b}^{\mathrm{R}} M_{6b(3^*)} + dm_{4b}^{\mathrm{R}} dm_{4b(2^*)}^{\mathrm{UV}} M_{2^*} + dm_{4b}^{\mathrm{R}} dm_{2^*}^{\mathrm{UV}} M_{4b(2^*)} \\
&+ dm_2^{\mathrm{UV}} dm_{2^*}^{\mathrm{R}} M_{6b(3^*)} + B_2^{\mathrm{UV}} dm_{2(1')}^{\mathrm{R}} M_{6b(3^*)} - dm_{4b}^{\mathrm{R}} dm_{2^*}^{\mathrm{UV}} dm_{2^*}^{\mathrm{UV}} M_{2^*} \\
&- dm_2^{\mathrm{UV}} dm_{2^*}^{\mathrm{R}} dm_{4b(2^*)}^{\mathrm{UV}} M_{2^*} - B_2^{\mathrm{UV}} dm_{2(1')}^{\mathrm{R}} dm_{4b(2^*)}^{\mathrm{UV}} M_{2^*} \\
&- dm_2^{\mathrm{UV}} dm_{2^*}^{\mathrm{R}} dm_{2^*}^{\mathrm{UV}} M_{4b(2^*)} - B_2^{\mathrm{UV}} dm_{2(1')}^{\mathrm{R}} dm_{2^*}^{\mathrm{UV}} M_{4b(2^*)} \\
&+ dm_2^{\mathrm{UV}} dm_{2^*}^{\mathrm{R}} dm_{2^*}^{\mathrm{UV}} dm_{2^*}^{\mathrm{UV}} M_{2^*} + B_2^{\mathrm{UV}} dm_{2(1')}^{\mathrm{R}} dm_{2^*}^{\mathrm{UV}} dm_{2^*}^{\mathrm{UV}} M_{2^*}
\end{aligned}
$$

$$
\begin{aligned}
&- M_{4b}L^{\mathrm{R}}_{6b3v} + M_{4b}L^{\mathrm{UV}}_{4b2v}L^{\mathrm{R}}_{2v} + M_{4b}L^{\mathrm{UV}}_{2v}L^{\mathrm{R}}_{4b2v} + dm_2^{\mathrm{UV}}M_{2^*}L^{\mathrm{R}}_{6b3v}\\
&+ B_2^{\mathrm{UV}}M_2L^{\mathrm{R}}_{6b3v} - M_{4b}L^{\mathrm{UV}}_{2v}L^{\mathrm{UV}}_{2v}L^{\mathrm{R}}_{2v} - dm_2^{\mathrm{UV}}M_{2^*}L^{\mathrm{UV}}_{4b2v}L^{\mathrm{R}}_{2v}\\
&- B_2^{\mathrm{UV}}M_2L^{\mathrm{UV}}_{4b2v}L^{\mathrm{R}}_{2v} - dm_2^{\mathrm{UV}}M_{2^*}L^{\mathrm{UV}}_{2v}L^{\mathrm{R}}_{4b2v} - B_2^{\mathrm{UV}}M_2L^{\mathrm{UV}}_{2v}L^{\mathrm{R}}_{4b2v}\\
&+ dm_2^{\mathrm{UV}}M_{2^*}L^{\mathrm{UV}}_{2v}L^{\mathrm{UV}}_{2v}L^{\mathrm{R}}_{2v} + B_2^{\mathrm{UV}}M_2L^{\mathrm{UV}}_{2v}L^{\mathrm{UV}}_{2v}L^{\mathrm{R}}_{2v} - M_2L^{\mathrm{R}}_{474v}\\
&+ M_2L^{\mathrm{UV}}_{6b3v}L^{\mathrm{R}}_{2v} + M_2L^{\mathrm{UV}}_{4b2v}L^{\mathrm{R}}_{4b2v} + M_2L^{\mathrm{UV}}_{2v}L^{\mathrm{R}}_{6b3v}\\
&- M_2L^{\mathrm{UV}}_{4b2v}L^{\mathrm{UV}}_{2v}L^{\mathrm{R}}_{2v} - M_2L^{\mathrm{UV}}_{2v}L^{\mathrm{UV}}_{4b2v}L^{\mathrm{R}}_{2v} - M_2L^{\mathrm{UV}}_{2v}L^{\mathrm{UV}}_{2v}L^{\mathrm{R}}_{4b2v}\\
&+ M_2L^{\mathrm{UV}}_{2v}L^{\mathrm{UV}}_{2v}L^{\mathrm{UV}}_{2v}L^{\mathrm{R}}_{2v} + dm^{\mathrm{R}}_{6b}dm^{\mathrm{R}}_{2^*}M_{2^*} - dm_{4b}^{\mathrm{UV}}dm^{\mathrm{R}}_{2^*}dm^{\mathrm{R}}_{2^*}M_{2^*}\\
&- B_{4b}^{\mathrm{UV}}dm^{\mathrm{R}}_{2(1')}dm^{\mathrm{R}}_{2^*}M_{2^*} - dm_2^{\mathrm{UV}}dm^{\mathrm{R}}_{4b(2^*)}dm^{\mathrm{R}}_{2^*}M_{2^*}\\
&- B_2^{\mathrm{UV}}dm^{\mathrm{R}}_{4b(2')}dm^{\mathrm{R}}_{2^*}M_{2^*} + dm_2^{\mathrm{UV}}dm^{\mathrm{UV}}_{2^*}dm^{\mathrm{R}}_{2^*}dm^{\mathrm{R}}_{2^*}M_{2^*}\\
&+ B_2^{\mathrm{UV}}dm^{\mathrm{UV}}_{2(1')}dm^{\mathrm{R}}_{2^*}dm^{\mathrm{R}}_{2^*}M_{2^*} + B_2^{\mathrm{UV}}B^{\mathrm{UV}}_{2(1')}dm^{\mathrm{R}}_{2(1')}dm^{\mathrm{R}}_{2^*}M_{2^*}\\
&+ dm^{\mathrm{R}}_{6b}M_{2^*}L^{\mathrm{R}}_{2v} - dm_{4b}^{\mathrm{UV}}dm^{\mathrm{R}}_{2^*}M_{2^*}L^{\mathrm{R}}_{2v} - B_{4b}^{\mathrm{UV}}dm^{\mathrm{R}}_{2(1')}M_{2^*}L^{\mathrm{R}}_{2v}\\
&- dm_2^{\mathrm{UV}}dm^{\mathrm{R}}_{4b(2^*)}M_{2^*}L^{\mathrm{R}}_{2v} - B_2^{\mathrm{UV}}dm^{\mathrm{R}}_{4b(2')}M_{2^*}L^{\mathrm{R}}_{2v}\\
&+ dm_2^{\mathrm{UV}}dm^{\mathrm{UV}}_{2^*}dm^{\mathrm{R}}_{2^*}M_{2^*}L^{\mathrm{R}}_{2v} + B_2^{\mathrm{UV}}dm^{\mathrm{UV}}_{2(1')}dm^{\mathrm{R}}_{2^*}M_{2^*}L^{\mathrm{R}}_{2v}\\
&+ B_2^{\mathrm{UV}}B^{\mathrm{UV}}_{2(1')}dm^{\mathrm{R}}_{2(1')}M_{2^*}L^{\mathrm{R}}_{2v} + M_{6b}L^{\mathrm{R}}_{2v}L^{\mathrm{R}}_{2v} - dm_{4b}^{\mathrm{UV}}M_{2^*}L^{\mathrm{R}}_{2v}L^{\mathrm{R}}_{2v}\\
&- B_{4b}^{\mathrm{UV}}M_2L^{\mathrm{R}}_{2v}L^{\mathrm{R}}_{2v} - dm_2^{\mathrm{UV}}M_{4b(2^*)}L^{\mathrm{R}}_{2v}L^{\mathrm{R}}_{2v} - B_2^{\mathrm{UV}}M_{4b}L^{\mathrm{R}}_{2v}L^{\mathrm{R}}_{2v}\\
&+ dm_2^{\mathrm{UV}}dm^{\mathrm{UV}}_{2^*}M_{2^*}L^{\mathrm{R}}_{2v}L^{\mathrm{R}}_{2v} + B_2^{\mathrm{UV}}dm^{\mathrm{UV}}_{2(1')}M_{2^*}L^{\mathrm{R}}_{2v}L^{\mathrm{R}}_{2v}\\
&+ B_2^{\mathrm{UV}}B^{\mathrm{UV}}_{2(1')}M_2L^{\mathrm{R}}_{2v}L^{\mathrm{R}}_{2v} + dm^{\mathrm{R}}_{4b}dm^{\mathrm{R}}_{4b(2^*)}M_{2^*} - dm^{\mathrm{R}}_{4b}dm^{\mathrm{UV}}_{2^*}dm^{\mathrm{R}}_{2^*}M_{2^*}\\
&- dm_2^{\mathrm{UV}}dm^{\mathrm{R}}_{2^*}dm^{\mathrm{R}}_{4b(2^*)}M_{2^*} - B_2^{\mathrm{UV}}dm^{\mathrm{R}}_{2(1')}dm^{\mathrm{R}}_{4b(2^*)}M_{2^*}\\
&+ dm_2^{\mathrm{UV}}dm^{\mathrm{R}}_{2^*}dm^{\mathrm{UV}}_{2^*}dm^{\mathrm{R}}_{2^*}M_{2^*} + B_2^{\mathrm{UV}}dm^{\mathrm{R}}_{2(1')}dm^{\mathrm{UV}}_{2^*}dm^{\mathrm{R}}_{2^*}M_{2^*}\\
&+ dm^{\mathrm{R}}_{4b}M_{4b(2^*)}L^{\mathrm{R}}_{2v} - dm^{\mathrm{R}}_{4b}dm^{\mathrm{UV}}_{2^*}M_{2^*}L^{\mathrm{R}}_{2v}\\
&- dm_2^{\mathrm{UV}}dm^{\mathrm{R}}_{2^*}M_{4b(2^*)}L^{\mathrm{R}}_{2v} - B_2^{\mathrm{UV}}dm^{\mathrm{R}}_{2(1')}M_{4b(2^*)}L^{\mathrm{R}}_{2v}\\
&+ dm_2^{\mathrm{UV}}dm^{\mathrm{R}}_{2^*}dm^{\mathrm{UV}}_{2^*}M_{2^*}L^{\mathrm{R}}_{2v} + B_2^{\mathrm{UV}}dm^{\mathrm{R}}_{2(1')}dm^{\mathrm{UV}}_{2^*}M_{2^*}L^{\mathrm{R}}_{2v}\\
&+ M_{4b}L^{\mathrm{R}}_{4b2v}L^{\mathrm{R}}_{2v} - M_{4b}L^{\mathrm{UV}}_{2v}L^{\mathrm{R}}_{2v}L^{\mathrm{R}}_{2v} - dm_2^{\mathrm{UV}}M_{2^*}L^{\mathrm{R}}_{4b2v}L^{\mathrm{R}}_{2v}\\
&- B_2^{\mathrm{UV}}M_2L^{\mathrm{R}}_{4b2v}L^{\mathrm{R}}_{2v} + dm_2^{\mathrm{UV}}M_{2^*}L^{\mathrm{UV}}_{2v}L^{\mathrm{R}}_{2v}L^{\mathrm{R}}_{2v}\\
&- dm^{\mathrm{R}}_{4b}dm^{\mathrm{R}}_{2^*}dm^{\mathrm{UV}}_{2^*}M_{2^*} + B_2^{\mathrm{UV}}M_2L^{\mathrm{UV}}_{2v}L^{\mathrm{R}}_{2v}L^{\mathrm{R}}_{2v} + M_2L^{\mathrm{R}}_{6b3v}L^{\mathrm{R}}_{2v}\\
&- M_2L^{\mathrm{UV}}_{4b2v}L^{\mathrm{R}}_{2v}L^{\mathrm{R}}_{2v} - M_2L^{\mathrm{UV}}_{2v}L^{\mathrm{R}}_{4b2v}L^{\mathrm{R}}_{2v}\\
&+ M_2L^{\mathrm{UV}}_{2v}L^{\mathrm{UV}}_{2v}L^{\mathrm{R}}_{2v}L^{\mathrm{R}}_{2v} + dm^{\mathrm{R}}_{4b}dm^{\mathrm{R}}_{2^*}M_{4b(2^*)}
\end{aligned}
$$

$$
\begin{aligned}
&- dm_2^{\rm UV} dm_{2^*}^{\rm R} dm_{2^*}^{\rm R} M_{4b(2^*)} - B_2^{\rm UV} dm_{2(1')}^{\rm R} dm_{2^*}^{\rm R} M_{4b(2^*)} \\
&+ dm_2^{\rm UV} dm_{2^*}^{\rm R} dm_{2^*}^{\rm R} dm_{2^*}^{\rm UV} M_{2^*} + B_2^{\rm UV} dm_{2(1')}^{\rm R} dm_{2^*}^{\rm R} dm_{2^*}^{\rm UV} M_{2^*} \\
&+ dm_{4b}^{\rm R} M_{2^*} L_{4b2v}^{\rm R} - dm_{4b}^{\rm R} M_{2^*} L_{2v}^{\rm UV} L_{2v}^{\rm R} - dm_2^{\rm UV} dm_{2^*}^{\rm R} M_{2^*} L_{4b2v}^{\rm R} \\
&- B_2^{\rm UV} dm_{2(1')}^{\rm R} M_{2^*} L_{4b2v}^{\rm R} + dm_2^{\rm UV} dm_{2^*}^{\rm R} M_{2^*} L_{2v}^{\rm UV} L_{2v}^{\rm R} \\
&+ B_2^{\rm UV} dm_{2(1')}^{\rm R} M_{2^*} L_{2v}^{\rm UV} L_{2v}^{\rm R} + M_{4b} L_{2v}^{\rm R} L_{4b2v}^{\rm R} \\
&- M_{4b} L_{2v}^{\rm R} L_{2v}^{\rm UV} L_{2v}^{\rm R} - dm_2^{\rm UV} M_{2^*} L_{2v}^{\rm R} L_{4b2v}^{\rm R} - B_2^{\rm UV} M_2 L_{2v}^{\rm R} L_{4b2v}^{\rm R} \\
&+ dm_2^{\rm UV} M_{2^*} L_{2v}^{\rm R} L_{2v}^{\rm UV} L_{2v}^{\rm R} + B_2^{\rm UV} M_2 L_{2v}^{\rm R} L_{2v}^{\rm UV} L_{2v}^{\rm R} \\
&+ M_2 L_{4b2v}^{\rm R} L_{4b2v}^{\rm R} - M_2 L_{4b2v}^{\rm R} L_{2v}^{\rm UV} L_{2v}^{\rm R} - M_2 L_{2v}^{\rm UV} L_{2v}^{\rm R} L_{4b2v}^{\rm R} \\
&+ M_2 L_{2v}^{\rm UV} L_{2v}^{\rm R} L_{2v}^{\rm UV} L_{2v}^{\rm R} + M_2 L_{2v}^{\rm R} L_{6b3v}^{\rm R} - M_2 L_{2v}^{\rm R} L_{4b2v}^{\rm UV} L_{2v}^{\rm R} \\
&- M_2 L_{2v}^{\rm R} L_{2v}^{\rm UV} L_{4b2v}^{\rm R} + M_2 L_{2v}^{\rm R} L_{2v}^{\rm UV} L_{2v}^{\rm UV} L_{2v}^{\rm R} - dm_{4b}^{\rm R} dm_{2^*}^{\rm R} dm_{2^*}^{\rm R} M_{2^*} \\
&+ dm_2^{\rm UV} dm_{2^*}^{\rm R} dm_{2^*}^{\rm R} dm_{2^*}^{\rm R} M_{2^*} + B_2^{\rm UV} dm_{2(1')}^{\rm R} dm_{2^*}^{\rm R} dm_{2^*}^{\rm R} M_{2^*} \\
&- dm_{4b}^{\rm R} dm_{2^*}^{\rm R} M_{2^*} L_{2v}^{\rm R} + dm_2^{\rm UV} dm_{2^*}^{\rm R} dm_{2^*}^{\rm R} M_{2^*} L_{2v}^{\rm R} \\
&+ B_2^{\rm UV} dm_{2(1')}^{\rm R} dm_{2^*}^{\rm R} M_{2^*} L_{2v}^{\rm R} - dm_{4b}^{\rm R} M_{2^*} L_{2v}^{\rm R} L_{2v}^{\rm R} \\
&+ dm_2^{\rm UV} dm_{2^*}^{\rm R} M_{2^*} L_{2v}^{\rm R} L_{2v}^{\rm R} + B_2^{\rm UV} dm_{2(1')}^{\rm R} M_{2^*} L_{2v}^{\rm R} L_{2v}^{\rm R} \\
&- M_{4b} L_{2v}^{\rm R} L_{2v}^{\rm R} L_{2v}^{\rm R} + dm_2^{\rm UV} M_{2^*} L_{2v}^{\rm R} L_{2v}^{\rm R} L_{2v}^{\rm R} + B_2^{\rm UV} M_2 L_{2v}^{\rm R} L_{2v}^{\rm R} L_{2v}^{\rm R} \\
&- M_2 L_{4b2v}^{\rm R} L_{2v}^{\rm R} L_{2v}^{\rm R} + M_2 L_{2v}^{\rm UV} L_{2v}^{\rm R} L_{2v}^{\rm R} L_{2v}^{\rm R} - M_2 L_{2v}^{\rm R} L_{4b2v}^{\rm R} L_{2v}^{\rm R} \\
&+ M_2 L_{2v}^{\rm R} L_{2v}^{\rm UV} L_{2v}^{\rm R} L_{2v}^{\rm R} - M_2 L_{2v}^{\rm R} L_{2v}^{\rm R} L_{4b2v}^{\rm R} \\
&+ M_2 L_{2v}^{\rm R} L_{2v}^{\rm R} L_{2v}^{\rm UV} L_{2v}^{\rm R} + M_2 L_{2v}^{\rm R} L_{2v}^{\rm R} L_{2v}^{\rm R} L_{2v}^{\rm R} \,. \qquad (39)
\end{aligned}
$$

### 4.10. *Integration by VEGAS*

As is seen from Eq. (33), Feynman integrals of Set V are defined on a hyperplane

$$\sum_{i=1}^{14} z_i = 1 \qquad (40)$$

in a 14-dimensional space. However, we perform numerical integration by VEGAS[65] over a 13-dimensional unit cube onto which Feynman parameters are mapped. There are infinitely many ways to choose this mapping, but it is useful to choose the largest sum of Feynman parameters that vanishes at the singularity of the integrand as one to be mapped onto an integration variable. Being a universal code, GENCODE*N* is not optimized for individual integrals. However, results of initial iterations by VEGAS provides a useful information about the structure of integrand. This information is used to improve the convergence of iteration process.

The results of numerical integration by VEGAS obtained by early 2012 and used as the input for the preliminary report[52] are listed in Tables 1 and 2. The first column of these tables lists the names of diagrams. The second column specifies the order in which the photon propagators connect the vertices of the electron line. The third column lists the values and their uncertainties evaluated by VEGAS. The columns 4–6 and 7–9 repeat the same identifications as those of the first three columns.

The preliminary value $\Delta M_{10}$[Set V], which is the sum of all integrals listed in Tables 1 and 2, is

$$\Delta M_{10}\ [\text{Set V}] = 4.877\ (570)\,. \tag{41}$$

Since the preliminary result was published, we have been reevaluating Set V diagrams for various choices of integration variables. The comparison of old and new evaluations suggests that estimated uncertainties of some integrals in Tables 1 and 2 were overly optimistic due to poor choice of mappings in the old calculation. An appropriate remapping helps remedy this problem. This work is still in progress. The new result will be reported shortly.

### 4.11. *Some information on running Set V*

GENCODE$N$ takes about 2 to 20 minutes to generate FORTRAN code for each diagram on a MacBook Pro. Typical integrand consists of about 90,000 lines of FORTRAN code occupying more than 5 Megabytes.

Evaluation in real*8 with $10^7$ sampling points iterated 100 times takes 2 hours on 32 cores of the Intel Xeon computer. Evaluation in real*16 is about 10 times slower.

### 4.12. *Residual renormalization*

Integrals in these tables are UV- and IR-finite. But they are not the standard renormalized amplitudes. Finite adjustment, called residual renormalization, must be made to compare with the observed $g-2$. Residual renormalization of all diagrams of Set V requires a systematic handling of 13,150 integrals.

Fortunately, residual terms can be organized into 16 terms whose structures are readily recognizable in terms of lower-order quantities:

$$\begin{aligned}
A_1^{(10)}\ [\text{Set V}] = {} & \Delta M_{10}[\text{Set V}] + \Delta M_8(-7\Delta LB_2) \\
& + \Delta M_6(-5\Delta LB_4 + 20(\Delta LB_2)^2) \\
& + \Delta M_4(-3\Delta LB_6 + 24\Delta LB_2\Delta LB_4 8(\Delta LB_2)^3 + 2\Delta L_{2^*}\Delta\delta m_4) \\
& + \Delta M_2(-\Delta LB_8 + 4(\Delta LB_4)^2 + 8\Delta LB_2\Delta LB_6 - 28(\Delta LB_2)^2\Delta LB_4 \\
& + 14(\Delta LB_2)^4 + 2\Delta L_{2^*}\Delta\delta m_6 - 2\Delta L_{2^*}\Delta\delta m_{2^*}\Delta\delta m_4 \\
& - 16\Delta L_{2^*}\Delta LB_2\Delta\delta m_4 + \Delta L_{4^*}\Delta\delta m_4)\,,
\end{aligned} \tag{42}$$

Table 1. Diagrams X001–X195 of Set V evaluated by VEGAS.

| | | | | | | | | |
|---|---|---|---|---|---|---|---|---|
| X001 | *abacbdcede* | −0.2981 (327) | X002 | *abaccddebe* | −5.9775 (447) | X003 | *abacdbcede* | −0.1142 (94) |
| X004 | *abacdcdebe* | 5.1244 (446) | X005 | *abacddbece* | 1.1401 (377) | X006 | *abacddcebe* | −5.2927 (432) |
| X007 | *abbcadceed* | −3.4755 (441) | X008 | *abbccddeea* | −16.5121 (447) | X009 | *abbcdaceed* | −3.1068 (157) |
| X010 | *abbcdcdeea* | 11.2581 (463) | X011 | *abbcddaeec* | 6.0519 (398) | X012 | *abbcddceea* | −9.3202 (304) |
| X013 | *abcabdecde* | −1.3540 (38) | X014 | *abcacdedbe* | 0.7833 (141) | X015 | *abcadbecde* | 2.1020 (19) |
| X016 | *abcadcedbe* | −0.9609 (19) | X017 | *abcaddebce* | 0.5174 (62) | X018 | *abcaddecbe* | 0.0579 (69) |
| X019 | *abcbadeced* | 1.2183 (139) | X020 | *abcbcdedea* | −8.1589 (447) | X021 | *abcbdaeced* | −0.2967 (48) |
| X022 | *abcbdcedea* | 0.9382 (433) | X023 | *abcbddeaec* | 0.6047 (417) | X024 | *abcbddecea* | −6.1010 (426) |
| X025 | *abccadeebd* | −0.7824 (411) | X026 | *abccbdeeda* | −7.8186 (336) | X027 | *abccdaeebd* | −2.3190 (315) |
| X028 | *abccdbeeda* | 4.5634 (445) | X029 | *abccddeeab* | 6.8839 (333) | X030 | *abccddeeba* | −12.6108 (385) |
| X031 | *abcdaebcde* | 2.2932 (28) | X032 | *abcdaecdbe* | −0.2427 (12) | X033 | *abcdaedbce* | −1.3771 (14) |
| X034 | *abcdaedcbe* | 1.2539 (20) | X035 | *abcdbeaced* | −0.5838 (14) | X036 | *abcdbecdea* | 0.2473 (63) |
| X037 | *abcdbedaec* | −0.7417 (19) | X038 | *abcdbedcea* | −0.2811 (49) | X039 | *abcdceaebd* | 0.3164 (44) |
| X040 | *abcdcebeda* | 1.4835 (313) | X041 | *abcdcedeab* | 3.1073 (222) | X042 | *abcdcedeba* | −4.1234 (417) |
| X043 | *abcddeeabc* | −2.8829 (356) | X044 | *abcddeebca* | 4.4462 (399) | X045 | *abcddeecab* | 3.4311 (323) |
| X046 | *abcddeecba* | −7.7360 (445) | X047 | *abcdeabcde* | −4.4551 (32) | X048 | *abcdeacdbe* | −0.8051 (16) |
| X049 | *abcdeadbce* | −0.0295 (13) | X050 | *abcdeadcbe* | −1.2222 (17) | X051 | *abcdebaced* | −0.1733 (20) |
| X052 | *abcdebcdea* | 0.9875 (93) | X053 | *abcdebdaec* | 0.3646 (15) | X054 | *abcdebdcea* | −0.4924 (70) |
| X055 | *abcdecaebd* | −0.3634 (14) | X056 | *abcdecbeda* | −0.2408 (54) | X057 | *abcdecdeab* | 2.6504 (164) |
| X058 | *abcdecdeba* | −5.1538 (331) | X059 | *abcdedeabc* | 2.1860 (176) | X060 | *abcdedebca* | −3.2607 (426) |
| X061 | *abcdedecab* | −3.7959 (324) | X062 | *abcdedecba* | 5.9124 (427) | X063 | *abcdeeabcd* | 3.3563 (86) |
| X064 | *abcdeeacbd* | −0.2763 (69) | X065 | *abcdeebadc* | 0.1748 (54) | X066 | *abcdeebcda* | −3.5299 (395) |
| X067 | *abcdeecdab* | −1.6869 (194) | X068 | *abcdeecdba* | 2.7503 (435) | X069 | *abcdeedabc* | −1.1586 (259) |
| X070 | *abcdeedbca* | 3.2263 (328) | X071 | *abcdeedcab* | 3.6917 (214) | X072 | *abcdeedcba* | −5.5323 (425) |
| X073 | *abacbdceed* | 3.4045 (447) | X074 | *abacbddece* | 4.4123 (445) | X075 | *abacbddeec* | −8.1242 (446) |
| X076 | *abacbdecde* | −5.2424 (229) | X077 | *abacbdeced* | 3.2616 (443) | X078 | *abacbdedce* | 1.1136 (301) |
| X079 | *abacbdedec* | 5.3998 (416) | X080 | *abacbdeecd* | 0.4971 (439) | X081 | *abacbdeedc* | −5.6478 (447) |
| X082 | *abaccdbeed* | −8.4886 (469) | X083 | *abaccddeeb* | 18.7509 (458) | X084 | *abaccdebde* | 8.9855 (278) |
| X085 | *abaccdebed* | −2.2692 (446) | X086 | *abaccdedbe* | 0.5038 (442) | X087 | *abaccdedeb* | −16.5811 (452) |
| X088 | *abaccdeebd* | −5.2728 (449) | X089 | *abaccdeedb* | 12.6876 (446) | X090 | *abacdbceed* | 1.5108 (293) |
| X091 | *abacdbdece* | −1.6970 (384) | X092 | *abacdbdeec* | 2.1137 (423) | X093 | *abacdbecde* | −1.7604 (49) |
| X094 | *abacdbeced* | −1.0460 (99) | X095 | *abacdbedce* | 0.5791 (43) | X096 | *abacdbedec* | 1.2849 (179) |
| X097 | *abacdbeecd* | 5.0171 (208) | X098 | *abacdbeedc* | −1.9365 (369) | X099 | *abacdcbeed* | 3.0812 (433) |
| X100 | *abacdcdeeb* | −15.3117 (479) | X101 | *abacdcebde* | −0.2625 (92) | X102 | *abacdcebed* | −1.3912 (311) |
| X103 | *abacdcedbe* | 0.8229 (193) | X104 | *abacdcedeb* | 6.4562 (456) | X105 | *abacdceebd* | 3.0452 (449) |
| X106 | *abacdceedb* | −11.5612 (447) | X107 | *abacddbeec* | −4.6713 (460) | X108 | *abacddceeb* | 12.9649 (440) |
| X109 | *abacddebce* | 0.0220 (439) | X110 | *abacddebec* | 1.9408 (417) | X111 | *abacddecbe* | 3.3869 (266) |
| X112 | *abacddeceb* | −11.9000 (442) | X113 | *abacddeebc* | −4.4439 (398) | X114 | *abacddeecb* | 11.1001 (448) |
| X115 | *abacdebcde* | −0.5947 (64) | X116 | *abacdebced* | 1.8059 (49) | X117 | *abacdebdce* | 0.3232 (44) |
| X118 | *abacdebdec* | −3.2225 (105) | X119 | *abacdebecd* | −0.1055 (112) | X120 | *abacdebedc* | 1.7913 (158) |
| X121 | *abacdecbde* | −0.8630 (43) | X122 | *abacdecbed* | −0.7414 (41) | X123 | *abacdecdbe* | −3.3339 (74) |
| X124 | *abacdecdeb* | 11.5793 (252) | X125 | *abacdecebd* | 0.7481 (188) | X126 | *abacdecedb* | −1.5694 (404) |
| X127 | *abacdedbce* | 1.1349 (58) | X128 | *abacdedbec* | 0.5916 (128) | X129 | *abacdedcbe* | 1.4312 (123) |
| X130 | *abacdedceb* | −1.5371 (393) | X131 | *abacdedebc* | 3.1212 (440) | X132 | *abacdedecb* | −8.8080 (447) |
| X133 | *abacdeebcd* | 2.6477 (422) | X134 | *abacdeebdc* | −0.6214 (250) | X135 | *abacdeecbd* | 0.9115 (343) |
| X136 | *abacdeecdb* | −7.4962 (455) | X137 | *abacdeedbc* | −2.3942 (447) | X138 | *abacdeedcb* | 10.1296 (445) |
| X139 | *abbcaddece* | 14.8570 (466) | X140 | *abbcadeced* | −2.7429 (443) | X141 | *abbcadedec* | −12.5828 (469) |
| X142 | *abbcadeecd* | −1.5860 (455) | X143 | *abbcadeedc* | 10.3414 (433) | X144 | *abbccdedea* | 23.7224 (462) |
| X145 | *abbccdeeda* | −18.6493 (456) | X146 | *abbcdadeec* | −2.3052 (443) | X147 | *abbcdaeced* | 1.1276 (223) |
| X148 | *abbcdaedec* | −1.3144 (363) | X149 | *abbcdaeecd* | −8.3912 (308) | X150 | *abbcdaeedc* | 2.8833 (365) |
| X151 | *abbcdcedea* | −10.9285 (449) | X152 | *abbcdceeda* | 14.6605 (461) | X153 | *abbcddecea* | 14.8929 (458) |
| X154 | *abbcddeeca* | −20.5917 (460) | X155 | *abbcdeadec* | 4.9510 (225) | X156 | *abbcdeaedc* | −0.8152 (144) |
| X157 | *abbcdecdea* | −11.8522 (408) | X158 | *abbcdeceda* | 0.4578 (448) | X159 | *abbcdedcea* | 0.4289 (442) |
| X160 | *abbcdedeca* | 14.0646 (452) | X161 | *abbcdeecda* | 7.7606 (428) | X162 | *abbcdeedca* | −12.8160 (407) |
| X163 | *abcabdceed* | 6.8345 (415) | X164 | *abcabddeec* | −12.8746 (306) | X165 | *abcabdeced* | −2.1380 (113) |
| X166 | *abcabdedce* | −2.2856 (121) | X167 | *abcabdedec* | 12.1602 (337) | X168 | *abcabdeecd* | 3.4558 (267) |
| X169 | *abcabdeedc* | −6.9274 (247) | X170 | *abcacdbeed* | 0.2692 (417) | X171 | *abcacddeeb* | −2.6121 (428) |
| X172 | *abcacdebed* | 1.4301 (224) | X173 | *abcacdedeb* | −0.0043 (443) | X174 | *abcacdeebd* | 1.7405 (407) |
| X175 | *abcacdeedb* | −1.8412 (397) | X176 | *abcadbceed* | 0.7651 (184) | X177 | *abcadbdeec* | −0.0111 (352) |
| X178 | *abcadbeced* | 0.7079 (37) | X179 | *abcadbedce* | −0.4378 (34) | X180 | *abcadbedec* | 0.0242 (43) |
| X181 | *abcadbeecd* | −4.3571 (146) | X182 | *abcadbeedc* | 1.2875 (157) | X183 | *abcadcbeed* | −0.0179 (186) |
| X184 | *abcadcdeeb* | 0.2587 (290) | X185 | *abcadcebed* | −0.1313 (49) | X186 | *abcadcedeb* | 1.1634 (49) |
| X187 | *abcadceebd* | 1.2832 (128) | X188 | *abcadceedb* | 1.8185 (232) | X189 | *abcaddbeec* | −3.7335 (226) |
| X190 | *abcaddceeb* | −2.4993 (358) | X191 | *abcaddebec* | 0.1938 (245) | X192 | *abcaddeceb* | 2.4665 (438) |
| X193 | *abcaddeebc* | −4.2494 (175) | X194 | *abcaddeecb* | −0.6704 (233) | X195 | *abcadebcde* | −1.0665 (45) |

Table 2. Diagrams X196–X389 of Set V evaluated by VEGAS.

| | | | | | | | | |
|---|---|---|---|---|---|---|---|---|
| X196 | *abcadebced* | −2.0375 (28) | X197 | *abcadebdce* | −0.3870 (22) | X198 | *abcadebdec* | −2.3452 (27) |
| X199 | *abcadebecd* | 1.0493 (38) | X200 | *abcadebedc* | 0.0092 (42) | X201 | *abcadecbde* | −0.4877 (36) |
| X202 | *abcadecbed* | 1.9243 (29) | X203 | *abcadecdbe* | 0.9037 (23) | X204 | *abcadecdeb* | −1.9324 (38) |
| X205 | *abcadecebd* | −0.9038 (48) | X206 | *abcadecedb* | 1.6447 (65) | X207 | *abcadedbce* | 0.2894 (41) |
| X208 | *abcadedbec* | 0.5215 (40) | X209 | *abcadedcbe* | 0.1444 (40) | X210 | *abcadedceb* | 0.7653 (49) |
| X211 | *abcadedebc* | 5.1027 (347) | X212 | *abcadedecb* | −0.4404 (311) | X213 | *abcadeebcd* | −2.4132 (118) |
| X214 | *abcadeebdc* | 0.6646 (141) | X215 | *abcadeecbd* | 0.1151 (120) | X216 | *abcadeecdb* | −1.1993 (239) |
| X217 | *abcadeedbc* | −2.2244 (147) | X218 | *abcadeedcb* | −1.6499 (187) | X219 | *abcbaddeec* | 1.3745 (435) |
| X220 | *abcbadedec* | −2.5160 (431) | X221 | *abcbadeecd* | 0.6897 (346) | X222 | *abcbadeedc* | 0.8242 (385) |
| X223 | *abcbcdeeda* | 17.4877 (465) | X224 | *abcbdadeec* | 2.4650 (232) | X225 | *abcbdaedec* | 0.2928 (98) |
| X226 | *abcbdaeecd* | 1.0518 (231) | X227 | *abcbdaeedc* | 0.6828 (397) | X228 | *abcbdceeda* | −6.7936 (444) |
| X229 | *abcbddaeec* | −1.9854 (390) | X230 | *abcbddeeca* | 15.6662 (460) | X231 | *abcbdeadec* | −0.7467 (58) |
| X232 | *abcbdeaedc* | 0.4010 (115) | X233 | *abcbdecdea* | 8.5433 (433) | X234 | *abcbdeceda* | −2.4938 (441) |
| X235 | *abcbdedaec* | 0.7040 (99) | X236 | *abcbdedcea* | 2.0658 (380) | X237 | *abcbdedeca* | −12.9749 (447) |
| X238 | *abcbdeeadc* | 1.4003 (390) | X239 | *abcbdeecda* | −2.7763 (457) | X240 | *abcbdeedca* | 10.9697 (445) |
| X241 | *abccaddeeb* | 13.8333 (468) | X242 | *abccadedeb* | −10.4788 (450) | X243 | *abccadeedb* | 3.8849 (437) |
| X244 | *abccdadeeb* | −3.3016 (399) | X245 | *abccdaedeb* | 0.0824 (337) | X246 | *abccdaeedb* | −0.4379 (365) |
| X247 | *abccddaeeb* | 15.9411 (439) | X248 | *abccddeaeb* | −1.9503 (425) | X249 | *abccdeadeb* | 3.9940 (158) |
| X250 | *abccdeaedb* | −0.8949 (402) | X251 | *abccdedaeb* | −1.2982 (299) | X252 | *abccdedeab* | −10.9298 (449) |
| X253 | *abccdedeba* | 17.8409 (460) | X254 | *abccdeeadb* | 2.1746 (391) | X255 | *abccdeedab* | 8.1757 (439) |
| X256 | *abccdeedba* | −14.0448 (449) | X257 | *abcdabceed* | 5.6299 (259) | X258 | *abcdabdeec* | −0.4470 (167) |
| X259 | *abcdabeced* | 0.0160 (48) | X260 | *abcdabedec* | −0.4007 (35) | X261 | *abcdabeecd* | 6.3373 (172) |
| X262 | *abcdabeedc* | −2.2800 (140) | X263 | *abcdacbeed* | −2.7605 (143) | X264 | *abcdacdeeb* | 4.7945 (346) |
| X265 | *abcdacebed* | −0.6741 (33) | X266 | *abcdacedeb* | 0.1179 (48) | X267 | *abcdaceebd* | −0.6336 (98) |
| X268 | *abcdaceedb* | 0.1262 (190) | X269 | *abcdadbeec* | −0.6542 (308) | X270 | *abcdadceeb* | −1.6766 (213) |
| X271 | *abcdadebec* | 0.2415 (53) | X272 | *abcdadeceb* | −0.7339 (92) | X273 | *abcdadeebc* | −2.0001 (240) |
| X274 | *abcdadeecb* | 0.8899 (406) | X275 | *abcdaebced* | −0.7434 (44) | X276 | *abcdaebdce* | −0.5544 (28) |
| X277 | *abcdaebdec* | 2.7843 (15) | X278 | *abcdaebecd* | −0.1559 (44) | X279 | *abcdaebedc* | 0.8231 (38) |
| X280 | *abcdaecbed* | −1.0096 (46) | X281 | *abcdaecdeb* | −1.3724 (40) | X282 | *abcdaecebd* | 0.4841 (33) |
| X283 | *abcdaecedb* | −0.0505 (42) | X284 | *abcdaedbec* | −0.2711 (32) | X285 | *abcdaedceb* | 0.0169 (38) |
| X286 | *abcdaedebc* | 0.7775 (37) | X287 | *abcdaedecb* | 0.1874 (68) | X288 | *abcdaeebcd* | 4.1604 (151) |
| X289 | *abcdaeebdc* | −1.5135 (129) | X290 | *abcdaeecbd* | −3.7248 (117) | X291 | *abcdaeecdb* | 1.5878 (177) |
| X292 | *abcdaeedbc* | 0.9126 (149) | X293 | *abcdaeedcb* | −1.1657 (265) | X294 | *abcdbaceed* | −3.3322 (165) |
| X295 | *abcdbadeec* | 1.7876 (185) | X296 | *abcdbaeced* | 0.5448 (45) | X297 | *abcdbaedec* | −0.4792 (46) |
| X298 | *abcdbaeecd* | −1.8909 (115) | X299 | *abcdbaeedc* | −0.2647 (121) | X300 | *abcdbceeda* | −9.4223 (423) |
| X301 | *abcdbdaeec* | −1.3250 (172) | X302 | *abcdbdeeca* | −1.8517 (425) | X303 | *abcdbeadec* | 0.3213 (24) |
| X304 | *abcdbeaecd* | −0.3422 (48) | X305 | *abcdbeaedc* | 0.4619 (39) | X306 | *abcdbeceda* | 0.1582 (225) |
| X307 | *abcdbedeca* | −0.1151 (396) | X308 | *abcdbeeadc* | 1.8367 (145) | X309 | *abcdbeecda* | −4.2650 (375) |
| X310 | *abcdbeedca* | 0.2505 (354) | X311 | *abcdcabeed* | −0.4378 (277) | X312 | *abcdcadeeb* | −1.2052 (291) |
| X313 | *abcdcaebed* | 0.9513 (42) | X314 | *abcdcaedeb* | 0.7992 (70) | X315 | *abcdcaeebd* | −1.2886 (216) |
| X316 | *abcdcaeedb* | 0.1050 (337) | X317 | *abcdcbeeda* | 1.4321 (423) | X318 | *abcdcdaeeb* | −8.7818 (449) |
| X319 | *abcdcdeaeb* | 0.7092 (408) | X320 | *abcdceadeb* | 0.5585 (45) | X321 | *abcdceaedb* | −0.9154 (78) |
| X322 | *abcdcedaeb* | 0.9205 (32) | X323 | *abcdceeadb* | 0.0954 (330) | X324 | *abcdceedab* | −8.8013 (450) |
| X325 | *abcdceedba* | 11.5665 (451) | X326 | *abcddabeec* | −8.9926 (329) | X327 | *abcddaceeb* | 1.4952 (434) |
| X328 | *abcddaebec* | −0.2799 (191) | X329 | *abcddaeceb* | −0.8929 (251) | X330 | *abcddaeebc* | −4.9477 (177) |
| X331 | *abcddaeecb* | 4.6920 (273) | X332 | *abcddbaeec* | 3.0339 (341) | X333 | *abcddbeeca* | 6.7608 (448) |
| X334 | *abcddcaeeb* | 5.1876 (428) | X335 | *abcddceaeb* | −2.0382 (302) | X336 | *abcddeabec* | −0.7509 (76) |
| X337 | *abcddeaceb* | −1.1895 (143) | X338 | *abcddeaebc* | −1.8395 (208) | X339 | *abcddeaecb* | 0.4930 (283) |
| X340 | *abcddebeca* | −2.1646 (449) | X341 | *abcddecaeb* | 1.8004 (136) | X342 | *abcddeeacb* | 2.5993 (172) |
| X343 | *abcdeabced* | 3.8805 (28) | X344 | *abcdeabdce* | 3.4147 (36) | X345 | *abcdeabdec* | −1.0015 (24) |
| X346 | *abcdeabecd* | 0.2844 (36) | X347 | *abcdeabedc* | −2.6792 (28) | X348 | *abcdeacbed* | −0.4859 (37) |
| X349 | *abcdeacdeb* | 2.0816 (43) | X350 | *abcdeacebd* | 1.4548 (23) | X351 | *abcdeacedb* | 0.2449 (34) |
| X352 | *abcdeadbec* | −0.1319 (25) | X353 | *abcdeadceb* | 0.1884 (25) | X354 | *abcdeadebc* | −2.0375 (24) |
| X355 | *abcdeadecb* | −1.0637 (30) | X356 | *abcdeaebcd* | 2.0708 (48) | X357 | *abcdeaebdc* | 0.3634 (36) |
| X358 | *abcdeaecbd* | 0.0333 (42) | X359 | *abcdeaecdb* | −0.1515 (45) | X360 | *abcdeaedbc* | −0.4709 (41) |
| X361 | *abcdeaedcb* | 2.5319 (64) | X362 | *abcdebadec* | −0.5660 (35) | X363 | *abcdebaecd* | −2.3416 (22) |
| X364 | *abcdebaedc* | 2.3899 (21) | X365 | *abcdebceda* | 0.4884 (114) | X366 | *abcdebdeca* | 5.6077 (221) |
| X367 | *abcdebeadc* | −0.7180 (49) | X368 | *abcdebecda* | −0.2878 (179) | X369 | *abcdebedca* | −3.2062 (395) |
| X370 | *abcdecadeb* | −1.4791 (45) | X371 | *abcdecaedb* | −0.0074 (41) | X372 | *abcdecdaeb* | −1.2875 (25) |
| X373 | *abcdeceadb* | 0.5684 (39) | X374 | *abcdecedab* | 0.9210 (437) | X375 | *abcdecedba* | 1.0206 (374) |
| X376 | *abcdedabec* | 1.0369 (33) | X377 | *abcdedaceb* | 0.4192 (36) | X378 | *abcdedaebc* | 1.3081 (33) |
| X379 | *abcdedaecb* | −0.3402 (52) | X380 | *abcdedbeca* | −0.9354 (359) | X381 | *abcdedcaeb* | 1.0677 (37) |
| X382 | *abcdedeacb* | −1.6457 (389) | X383 | *abcdeeabdc* | −4.7039 (136) | X384 | *abcdeeacdb* | 1.9230 (183) |
| X385 | *abcdeeadbc* | −0.6982 (140) | X386 | *abcdeeadcb* | 0.7383 (243) | X387 | *abcdeebdca* | 1.9526 (316) |
| X388 | *abcdeecadb* | −0.3893 (199) | X389 | *abcdeedacb* | −0.0490 (149) | | | |

Table 3. Residual renormalization constants used to calculate $a_e^{(10)}$ [Set V].

| | | | |
|---|---|---|---|
| $\Delta M_8$ | 1.738 67 (206) | $\Delta M_6$ | 0.425 814 (7) |
| $\Delta M_4$ | 0.030 833 612 ... | $M_2$ | 0.5 |
| $\Delta LB_8$ | 2.101 9 (719) | $\Delta LB_6$ | 0.100 81 (21) |
| $\Delta LB_4$ | 0.027 919 (13) | $\Delta LB_2$ | 0.75 |
| $\Delta L_{4^*}$ | −0.459 051 (62) | $\Delta L_{2^*}$ | −0.75 |
| $\Delta dm_6$ | −2.340 51 (38) | $\Delta dm_4$ | 1.906 340 (21) |
| $\Delta dm_{2^*}$ | −0.75 | | |

where $\Delta M_n$ is the finite part of the $n$th order magnetic moment, $\Delta LB_n$ is the sum of finite parts of the $n$th order vertex renormalization constant $\Delta L_n$ and the wave function renormalization constant $\Delta B_n$. $\Delta\delta m_n$ is the finite part of the $n$th order selfmass of the electron. $\Delta L_{n^*}$ is obtained from $\Delta L_n$ by insertion of 2-vertex in the electron line. All these quantities ($n \leq 8$) correspond to diagrams that have no closed electron loop.

Substituting the values of these quantities listed in Table 3 and the value of $\Delta M_{10}$ [Set V] from Eq. (41) in Eq. (42) we obtain

$$A_1^{(10)}\ [\text{Set V}] = 10.092\ (570)\,. \tag{43}$$

This is still very very preliminary. It is being upgraded.

### 4.13. *Collecting all tenth-order terms*

Automating codes for diagrams containing vacuum-polarization or light-by-light-scattering subdiagram are obtained by some modification of GENCODE$N$.[56,57] Their FORTRAN code becomes analytically exact when residual renormalization terms are included. No approximation is involved. The uncertainty of numerical value arises only from numerical integration carried out by VEGAS.

Contributions (as of 2012) of 32 gauge-invariant sets to $A_1^{(10)}$ and $A_2^{(10)}(m_e/m_\mu)$ are summarized in Table 4. Summing up these results, we obtain

$$A_1^{(10)} = 9.16\ (58)$$

and

$$A_2^{(10)}\left(\frac{m_e}{m_\mu}\right) = -0.003\ 82\ (39)\,,$$

which are reported in (24) and (25). $A_2^{(10)}(m_e/m_\tau)$ and $A_2^{(10)}(m_e/m_\mu, m_e/m_\tau)$ are also known. But, they are too small to affect our result at present.

## 5. What's Next?

- The value of $a_e(\text{th}:2012)$ given in (27) is the one we obtained before the summer of 2012. Primarily it showed that our computational renormalization scheme works

Table 4. Summary of contributions to the tenth-order lepton $g-2$ from 32 gauge-invariant subsets. $n_F$ is the number of vertex diagrams contributing to $A_1^{(10)}$. The numerical values of individual subsets were originally obtained in the references in the fifth column. The values of subsets I(d), I(f), II(a), II(b) and VI(c) in Ref. 66 are corrected in Ref. 52 as indicated by the asterisk.

| Set | $n_F$ | $A_1^{(10)}$ | $A_2^{(10)}(m_e/m_\mu)$ | Reference |
|---|---|---|---|---|
| I(a) | 1 | 0.000 470 94 (6) | 0.000 000 28 (1) | 66 |
| I(b) | 9 | 0.007 010 8 (7) | 0.000 001 88 (1) | 66 |
| I(c) | 9 | 0.023 468 (2) | 0.000 002 67 (1) | 66 |
| I(d) | 6 | 0.003 801 7 (5) | 0.000 005 46 (1) | 66* |
| I(e) | 30 | 0.010 296 (4) | 0.000 001 60 (1) | 66 |
| I(f) | 3 | 0.007 568 4 (20) | 0.000 047 54 (1) | 66* |
| I(g) | 9 | 0.028 569 (6) | 0.000 024 45 (1) | 68 |
| I(h) | 30 | 0.001 696 (13) | −0.000 010 14 (3) | 68 |
| I(i) | 105 | 0.017 47 (11) | 0.000 001 67 (2) | 57 |
| I(j) | 6 | 0.000 397 5 (18) | 0.000 002 41 (6) | 70 |
| II(a) | 24 | −0.109 495 (23) | −0.000 737 69 (95) | 66* |
| II(b) | 108 | −0.473 559 (84) | −0.000 645 62 (95) | 66* |
| II(c) | 36 | −0.116 489 (32) | −0.000 380 25 (46) | 70 |
| II(d) | 180 | −0.243 00 (29) | −0.000 098 17 (41) | 70 |
| II(e) | 180 | −1.344 9 (10) | −0.000 465 0 (40) | 69 |
| II(f) | 72 | −2.433 6 (15) | −0.005 868 (39) | 66 |
| III(a) | 300 | 2.127 33 (17) | 0.007 511 (11) | 57 |
| III(b) | 450 | 3.327 12 (45) | 0.002 794 (1) | 57 |
| III(c) | 390 | 4.921 (11) | 0.003 70 (36) | 73 |
| IV | 2072 | −7.7296 (48) | −0.011 36 (7) | 72 |
| V | 6354 | 10.09 (57) | 0 | 52 |
| VI(a) | 36 | 1.041 32 (19) | 0.006 152 (11) | 66 |
| VI(b) | 54 | 1.346 99 (28) | 0.001 778 9 (35) | 66 |
| VI(c) | 144 | −2.5289 (28) | −0.005 953 (59) | 66* |
| VI(d) | 492 | 1.8467 (70) | 0.001 276 (76) | 56 |
| VI(e) | 48 | −0.4312 (7) | −0.000 750 (8) | 66 |
| VI(f) | 180 | 0.7703 (22) | 0.000 033 (7) | 66 |
| VI(g) | 480 | −1.5904 (63) | −0.000 497 (29) | 56 |
| VI(h) | 630 | 0.1792 (39) | 0.000 045 (9) | 56 |
| VI(i) | 60 | −0.0438 (12) | −0.000 326 (1) | 66 |
| VI(j) | 54 | −0.2288 (18) | −0.000 127 (13) | 66 |
| VI(k) | 120 | 0.6802 (38) | 0.000 015 6 (40) | 66 |

in the tenth-order. It was published as a preliminary result, since its uncertainty is already several times smaller than the uncertainty of the measurement (2). We were well aware that uncertainties of many of the integrals might have been underestimated because of insufficient samplings of the integrands. For more than a year, since then, we have been reevaluating these integrals with various remappings and larger sampling statistics in order to obtain more reliable error estimates. We have already accumulated a lot of higher quality data, but it will take some more work before it is ready for publication.

- Although $A_1^{(8)}$ has been evaluated with uncertainty of 0.1%, it is at present the largest source of theoretical uncertainty. This will be improved by further work.
- Harvard group is building a new Penning trap with much smaller cavity. They also cool down the axial motion to the order of 100 milli Kelvin to make the electron/positron stay much longer in the ground state.
- $\alpha(Rb11)$ is derived from the formula

$$\alpha(\mathrm{Rb11}) = \left[\frac{2R_\infty}{c}\frac{m_{\mathrm{Rb}}}{m_e}\frac{h}{m_{\mathrm{Rb}}}\right]^{1/2}, \tag{44}$$

where[53,54,58]

$$\begin{aligned} c &= 299\ 792\ 458\ \mathrm{ms}^{-1} \quad (\text{exact by definition}), \\ m(^{87}\mathrm{Rb}) &= 86.909\ 180\ 535\ (10) \quad (\text{in atomic mass units}) \quad [1.2\times10^{-10}], \\ m_e &= 0.000\ 548\ 579\ 909\ 46\ (22) \quad [4.0\times10^{-10}], \\ R_\infty &= 10\ 973\ 731.568\ 539\ (55)\ m^{-1} \quad [5.0\times10^{-12}], \\ h/m(^{87}\mathrm{Rb}) &= 4.591\ 359\ 2729\ (57)\times10^{-9}\ \mathrm{m}^2\ \mathrm{s}^{-1} \quad [1.2\times10^{-9}]. \end{aligned} \tag{45}$$

The precision of $\alpha$(Rb11) is limited by the $h/m$ factor. They are going to improve measurement of $\alpha$ by means of Bose–Einstein condensation which may increase the number of coherent Rb atoms by three-orders of magnitude.

When all these improvements are realized, QED may be tested to 0.1 ppb.

## 6. Discussion

The discoverers of QED, such as Tomonaga[74] and Dyson,[75] regarded the renormalization as a jerry-built temporary fix to be replaced by something better.

Soon experiments showed that QED must be extended to include hadronic and weak interactions, which led to the SM. But jerry-built structure itself remained as the basic framework of SM.

SM itself is generally regarded as a temporary measure which must be modified to accommodate new physics. Such a modification is likely to come from experiments at high energy accelerators such as LHC.

As far as $a_e$ is concerned, however, the impact of possible new physics may not be straightforward. As a matter of fact, it might not have any detectable effect on the electron $g-2$.

The reason: Mass and charge in ordinary quantum mechanics (QM) cannot be correctly identified as physical mass and physical charge unless they include radiative corrections. Namely, for proper interpretation, the ordinary QM, by which these non-QED measurements of $\alpha$ are interpreted, must include radiative corrections as well as the effects of new physics.

Such a formulation exists for two-body bound systems, which is an exact adaptation of the renormalized QED (or SM) to bound states, unfortunately misnamed

NRQED. As far as I know, no attempt has been made thus far to extend it to $n$-body system, $n > 2$. But such an interpretation of many-body system in terms of physical mass and charge is unavoidable for proper interpretation of experiments.

If this argument hold water, $\alpha(a_e)$ must be identical with $\alpha$(Rb) or any other $\alpha$ measured in ordinary QM to any decimal point.

If several standards deviation develops in the next generation of test, it might be an indication that the jerry-built structure of QED or QM has at last started to break down after 66 years.

It would be really exciting if it is the harbinger of an entirely new physics beyond the framework of Quantum Mechanics.



## Acknowledgments

The author wishes to thank M. Nio for helping the preparation of this paper. This work is supported in part by the U.S. National Science Foundation under Grant NSF-PHY-0757868, and in part by the JSPS Grant-in-Aid for Scientific Research (c)23540331. He thanks RIKEN for the hospitality extended to him while a part of this work was carried out.

## References

1. P. A. M. Dirac, *Proc. R. Soc. London A* **117**, 610 (1928).
2. P. A. M. Dirac, *Proc. R. Soc. London A* **118**, 351 (1928).
3. D. Hanneke, S. Fogwell and G. Gabrielse, *Phys. Rev. Lett.* **100**, 120801 (2008).
4. D. Hanneke, S. F. Hoogerheide and G. Gabrielse, *Phys. Rev. A* **83**, 052122 (2011).
5. P. Kusch and H. M. Foley, *Phys. Rev.* **72**, 1256 (1947).
6. J. Schwinger, *Phys. Rev.* **73**, 416L (1948).
7. J. Schwinger, *Phys. Rev.* **75**, 898 (1949).
8. Z. Koba and S. Tomonaga, *Prog. Theor. Phys.* **2**, 218 (1947).
9. S. Tomonaga, *Phys. Rev.* **74**, 224 (1948).
10. J. Schwinger, *Phys. Rev.* **74**, 1439 (1948).
11. H. A. Bethe, *Phys. Rev.* **72**, 339 (1947).
12. R. Karplus and N. M. Kroll, *Phys. Rev.* **77**, 536 (1950).
13. P. A. Franken and S. Liebes, *Phys. Rev.* **104**, 1197 (1956).
14. A. Petermann, private communication.
15. A. Petermann, *Helv. Phys. Acta* **30**, 407 (1957).
16. C. M. Sommerfield, *Phys. Rev.* **107**, 328 (1957).
17. R. P. Feynman, *Phys. Rev.* **74**, 1430 (1948).
18. R. P. Feynman, *Phys. Rev.* **76**, 769 (1949).
19. F. J. Dyson, *Phys. Rev.* **75**, 486, 1736 (1949).
20. W. H. Louisell, R. W. Pidd and H. R. Crane, *Phys. Rev.* **91**, 475 (1953).
21. A. A. Shupp, R. W. Pidd and H. R. Crane, *Phys. Rev.* **121**, 1 (1961).
22. D. T. Wilkinson and H. R. Crane, *Phys. Rev.* **130**, 852 (1963).
23. J. C. Wesley and A. Rich, *Phys. Rev. A* **4**, 1341 (1971).
24. K. A. Milton, W. Y. Tsai and L. L. DeRaad, Jr., *Phys. Rev. D* **9**, 1809 (1974).
25. L. L. DeRaad, Jr., K. A. Milton and W. Y. Tsai, *Phys. Rev. D* **9**, 1814 (1974).
26. J. A. Mignaco and E. Remiddi, *Nuovo Cimento A* **60**, 519 (1969).
27. R. Barbieri and E. Remiddi, *Nucl. Phys. B* **90**, 233 (1975).

28. R. Barbieri, M. Caffo and E. Remiddi, *Phys. Lett. B* **57**, 460 (1975).
29. M. J. Levine and J. Wright, *Phys. Rev. D* **8**, 3171 (1973).
30. R. Carroll, *Phys. Rev. D* **12**, 2344 (1974).
31. J. Aldins, S. J. Brodsky, A. Dufner and T. Kinoshita, *Phys. Rev. Lett.* **23**, 441 (1969).
32. J. Aldins, S. J. Brodsky, A. Dufner and T. Kinoshita, *Phys. Rev. D* **1**, 2378 (1970).
33. T. Kinoshita, *Phys. Rev. Lett.* **75**, 4278 (1995).
34. S. Laporta and E. Remiddi, *Phys. Lett. B* **379**, 283 (1996).
35. H. H. Elend, *Phys. Lett.* **20**, 682 (1966).
36. M. A. Samuel and G. Li, *Phys. Rev. D* **44**, 3935 (1991).
37. G. Li, R. Mendell and M. A. Samuel, *Phys. Rev. D* **47**, 1723 (1993).
38. S. Laporta and E. Remiddi, *Phys. Lett. B* **301**, 440 (1993).
39. S. Laporta, *Nuovo Cimento A* **106**, 675 (1993).
40. M. Passera, *Phys. Rev. D* **75**, 013002 (2007).
41. D. Nomura and T. Teubner, *Nucl. Phys. B* **867**, 236 (2013).
42. J. Prades, E. de Rafael and A. Vainshtein, in *Lepton Dipole Moments*, eds. B. L. Roberts and W. J. Marciano (World Scientific, Singapore, 2009), pp. 303–319.
43. K. Fujikawa, B. W. Lee and A. I. Sanda, *Phys. Rev. D* **6**, 2923 (1972).
44. A. Czarnecki, B. Krause and W. J. Marciano, *Phys. Rev. Lett.* **76**, 3267 (1996).
45. M. Knecht, S. Peris, A. Perrottet and E. de Rafael, *J. High Energy Phys.* **11**, 003 (2002).
46. A. Czarnecki, W. J. Marciano and A. Vainshtein, *Phys. Rev. D* **67**, 073006 (2003).
47. P. J. Mohr, B. N. Taylor and D. B. Newell, *Rev. Mod. Phys.* **80**, 633 (2008).
48. H. G. Dehmelt, *Phys. Rev.* **109**, 381 (1958).
49. G. Graff, F. G. Major, R. W. H. Roeder and G. Werth, *Phys. Rev. Lett.* **21**, 340 (1968).
50. R. S. Van Dyck, P. B. Schwinberg and H. G. Dehmelt, *Phys. Rev. Lett.* **59**, 26 (1987).
51. T. Kinoshita and M. Nio, *Phys. Rev. D* **73**, 013003 (2006).
52. T. Aoyama, M. Hayakawa, T. Kinoshita and M. Nio, *Phys. Rev. Lett.* **109**, 111807 (2012).
53. R. Bouchendira, P. Clade, S. Guellati-Khelifa, F. Nez and F. Biraben, *Phys. Rev. Lett.* **106**, 080801 (2011).
54. P. J. Mohr, B. N. Taylor and D. B. Newell, *Rev. Mod. Phys.* **84**, 1527 (2012).
55. T. Aoyama, M. Hayakawa, T. Kinoshita and M. Nio, in preparation.
56. T. Aoyama, M. Hayakawa, T. Kinoshita and M. Nio, *Phys. Rev.* **82**, 113004 (2010).
57. T. Aoyama, M. Hayakawa, T. Kinoshita and M. Nio, *Phys. Rev.* **83**, 053003 (2011).
58. B. J. Mount, M. Redshaw and E. G. Myers, *Phys. Rev. A* **82**, 042513 (2010).
59. T. Aoyama, M. Hayakawa, T. Kinoshita and M. Nio, *Nucl. Phys. B* **740**, 138 (2006).
60. T. Aoyama, M. Hayakawa, T. Kinoshita and M. Nio, *Nucl. Phys. B* **796**, 184 (2008).
61. J. A. M. Vermaseren, New features of FORM, arXiv:math-ph/0010025.
62. P. Cvitanovic and T. Kinoshita, *Phys. Rev. D* **10**, 3978, 3991, 4007 (1974).
63. T. Aoyama, M. Hayakawa, T. Kinoshita and M. Nio, *Phys. Rev. D* **77**, 053012 (2008).
64. S. Laporta, *Phys. Lett. B* **328**, 522 (1994).
65. G. P. Lepage, *J. Comput. Phys.* **27**, 192 (1978).
66. T. Kinoshita and M. Nio, *Phys. Rev. D* **73**, 053007 (2006).
67. T. Aoyama, M. Hayakawa, T. Kinoshita, M. Nio and N. Watanabe, *Phys. Rev. D* **78**, 053005 (2008).

68. T. Aoyama, M. Hayakawa, T. Kinoshita and M. Nio, *Phys. Rev. D* **78**, 113006 (2008).
69. T. Aoyama, K. Asano, M. Hayakawa, T. Kinoshita, M. Nio and N. Watanabe, *Phys. Rev. D* **81**, 053009 (2010).
70. T. Aoyama, M. Hayakawa, T. Kinoshita and M. Nio, *Phys. Rev. D* **83**, 053002 (2011).
71. T. Aoyama, M. Hayakawa, T. Kinoshita and M. Nio, *Phys. Rev. D* **84**, 053003 (2011).
72. T. Aoyama, M. Hayakawa, T. Kinoshita and M. Nio, *Phys. Rev. D* **85**, 033007 (2012).
73. T. Aoyama, M. Hayakawa, T. Kinoshita and M. Nio, *Phys. Rev. D* **85**, 093013 (2012).
74. S. Tomonaga, private communication.
75. Letter of F. J. Dyson to G. Gabrielse, quoted in *Physics Today* (August 2006), p. 15.